

Introduction to Cluster Algebras

Chapter 7

(preliminary version)

SERGEY FOMIN

LAUREN WILLIAMS

ANDREI ZELEVINSKY

Preface

This is a preliminary draft of Chapter 7 of our forthcoming textbook *Introduction to cluster algebras*, joint with Andrei Zelevinsky (1953–2013).

Other chapters have been posted as

- [arXiv:1608.05735](#) (Chapters 1–3),
- [arXiv:1707.07190](#) (Chapters 4–5), and
- [arXiv:2008.09189](#) (Chapter 6).

We expect to post additional chapters in the not so distant future.

Anne Larsen and Raluca Vlad made a number of valuable suggestions that helped improve the quality of the manuscript. We are also grateful to Zenan Fu, Amal Mattoo, Hanna Mularczyk, and Ashley Wang for their comments on the earlier versions of this chapter, and for assistance with creating figures.

Our work was partially supported by the NSF grants DMS-1664722, DMS-1854512, and DMS-1854316, and by the Radcliffe Institute for Advanced Study.

Comments and suggestions are welcome.

Sergey Fomin
Lauren Williams

Contents

| | |
|---|----|
| Chapter 7. Plabic graphs | 1 |
| §7.1. Plabic graphs and their quivers | 3 |
| §7.2. Triangulations and wiring diagrams via plabic graphs | 7 |
| §7.3. Trivalent plabic graphs | 11 |
| §7.4. Trips. Reduced plabic graphs | 16 |
| §7.5. Triple diagrams and normal plabic graphs | 23 |
| §7.6. Minimal triple diagrams | 32 |
| §7.7. From minimal triple diagrams to reduced plabic graphs | 40 |
| §7.8. The bad features criterion | 44 |
| §7.9. Affine permutations | 47 |
| §7.10. Bridge decompositions | 51 |
| §7.11. Edge labels of reduced plabic graphs | 54 |
| §7.12. Face labels of reduced plabic graphs | 58 |
| §7.13. Grassmann necklaces and weakly separated collections | 62 |
| Bibliography | 67 |

Plabic graphs

In this chapter, we present the combinatorial machinery of *plabic graphs*, introduced and developed by A. Postnikov [21]. These are planar (unoriented) graphs with bicolored vertices satisfying some mild technical conditions. Plabic graphs can be transformed using certain *local moves*. A key observation is that each plabic graph gives rise to a quiver, so that local moves on plabic graphs translate into (a subclass of) quiver mutations.

Crucially, the combinatorics underlying several important classes of cluster structures that arise in applications fits into the plabic graphs framework. This in particular applies to the basic examples introduced in Chapter 1. More concretely, we show that the combinatorics of flips in triangulations of a convex polygon (resp., braid moves in wiring diagrams, either ordinary or double) can be entirely recast in the language of plabic graphs. In these and other examples, an important role is played by the subclass of *reduced* plabic graphs that are analogous to—and indeed generalize—reduced decompositions in symmetric groups.

D. Thurston’s *triple diagrams* [24] are closely related to plabic graphs. After making this connection precise and developing the machinery of triple diagrams, we use this machinery to establish the fundamental properties of reduced plabic graphs.

Plabic graphs and related combinatorics have arisen in the study of shallow water waves [16, 17] (via the KP equation) and in connection with scattering amplitudes in $\mathcal{N} = 4$ super Yang-Mills theory [2]. Constructions closely related to plabic graphs were studied by T. Kawamura [13] in the context of the topological theory of graph divides.

A reader interested exclusively in the combinatorics of plabic graphs can read this chapter independently of the previous ones. While we occasionally

refer to the combinatorial constructions introduced in Chapters 1–2, they are not relied upon in the development of the general theory of plabic graphs.

Cluster algebras as such do not appear in this chapter. On the other hand, reduced plabic graphs introduced herein will prominently feature in the upcoming study of cluster structures in Grassmannians and related varieties, see Chapter 8.

The structure of this chapter is as follows.

Section 7.1 introduces plabic graphs and their associated quivers.

In Section 7.2, we recast the combinatorics of triangulations of a polygon and (ordinary or double) wiring diagrams in the language of plabic graphs.

Section 7.3 discusses the version of the theory in which all internal vertices of plabic graphs are *trivalent*. (This version naturally arises in some applications, cf., e.g., [9].) As Section 7.3 is not strictly necessary for the sections that follow, it can be skipped if desired.

The important notions of a *trip*, a *trip permutation* and a *reduced plabic graph* are introduced in Section 7.4. Here we state (but do not prove) some key results, including the “fundamental theorem of reduced plabic graphs” which characterizes the move equivalence classes of reduced plabic graphs in terms of associated *decorated permutations*.

Section 7.5 introduces the basic notions of *triple diagrams*. We then show that triple diagrams are in bijection with *normal plabic graphs*.

In Section 7.6, we study *minimal* triple diagrams, largely following [24]. These diagrams can be viewed as counterparts of reduced plabic graphs.

In Section 7.7, we explain how to go between minimal triple diagrams and reduced plabic graphs. We then use this correspondence to prove the fundamental theorem of reduced plabic graphs.

In Section 7.8, we state and prove the *bad features criterion* that detects whether a plabic graph is reduced or not.

In Section 7.9, we describe a bijection between decorated permutations and a certain subclass of *affine permutations*.

In Section 7.10, a factorization algorithm for affine permutations is used to construct a family of reduced plabic graphs called *bridge decompositions*.

Section 7.11 discusses *edge labelings* of reduced plabic graphs and gives a particularly transparent *resonance criterion* for recognizing whether a plabic graph is reduced.

Section 7.12 introduces *face labelings* of reduced plabic graphs. In Section 7.13, we provide an intrinsic combinatorial characterization of collections of face labels that arise via this construction. Face labels will reappear in Chapter 8 in the study of cluster structures in Grassmannians.

7.1. Plabic graphs and their quivers

Definition 7.1.1. A *plabic* (planar bicolored) *graph* is a planar graph G embedded into a closed disk \mathbf{D} , such that:

- the embedding of G into \mathbf{D} is proper, i.e., the edges do not cross;
- each internal vertex is colored black or white;
- each internal vertex is connected by a path to some boundary vertex;
- the (uncolored) vertices lying on the boundary of \mathbf{D} are labeled $1, 2, \dots, b$ in clockwise order, for some positive integer b ;
- each of these b *boundary vertices* is incident to a single edge.

Loops and multiple edges are allowed.

We consider plabic graphs up to isotopy of the ambient disk \mathbf{D} fixing the disk's boundary. The *faces* of G are the connected components of the complement of G inside the ambient disk \mathbf{D} . A degree 1 internal vertex which is connected by an edge to a boundary vertex is called a *lollipop*.

Two examples of plabic graphs are shown in Figure 7.1. Many more examples appear throughout this chapter. In what follows, we will often omit the boundary of the ambient disk when drawing plabic graphs.

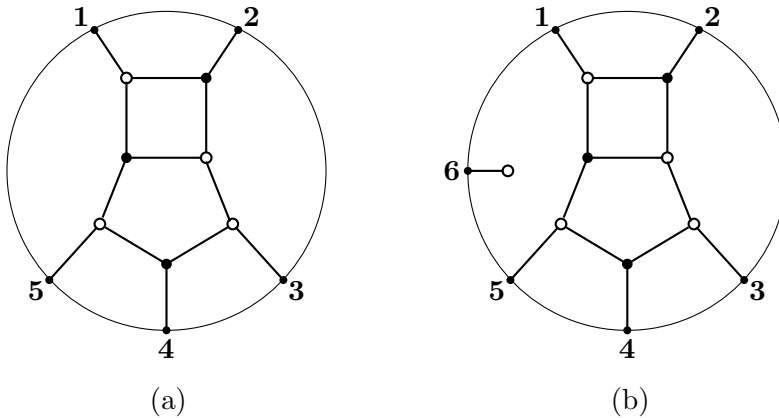


Figure 7.1. (a) A plabic graph G . (b) A plabic graph G' with a white lollipop.

Remark 7.1.2. Plabic graphs were introduced by A. Postnikov [21, Section 12], who used them to describe parametrizations of cells in totally non-negative Grassmannians. A closely related class of graphs was defined by T. Kawamura [13] in the context of the topological theory of *graph divides*. Our definition is very close to Postnikov's.

The key role in the theory of plabic graphs is played by a particular equivalence relation that is generated by a family of transformations called (*local*) *moves*.

Definition 7.1.3. We say that two plabic graphs G and G' are *move-equivalent*, and write $G \sim G'$, if G and G' can be related to each other via a sequence of the following *local moves*, denoted (M1), (M2), and (M3):

- (M1) (The *square move*) Change the colors of all vertices on the boundary of a quadrilateral face, provided these colors alternate and these vertices are trivalent. See Figure 7.2.

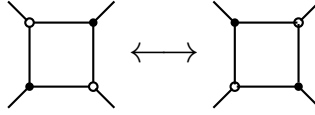


Figure 7.2. Move (M1) on plabic graphs.

- (M2) Remove a bivalent vertex (of any color) and merge the edges adjacent to it; or, conversely, insert a bivalent vertex in the middle of an edge. See Figure 7.3.

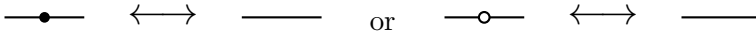


Figure 7.3. Move (M2) on plabic graphs.

- (M3) Contract an edge connecting two internal vertices of the same color; or split an internal vertex into two vertices of the same color joined by an edge. See Figure 7.4.

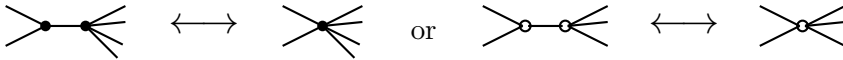


Figure 7.4. Move (M3) on plabic graphs. The number of “hanging” edges on either side can be any nonnegative integer.

We next explain how to associate a quiver to a plabic graph. This construction is closely related to the one presented in Definition 2.5.1.

Definition 7.1.4. The *quiver* $Q(G)$ associated to a plabic graph G is defined as follows. The vertices of $Q(G)$ are in one-to-one correspondence with the faces of G . A vertex of $Q(G)$ is declared mutable or frozen depending on whether the corresponding face is *internal* (i.e., disjoint from the boundary of \mathbf{D}) or not. The arrows of $Q(G)$ are constructed in the following way. Let e be an edge in G that connects a white vertex to a black vertex and separates two distinct faces, at least one of which is internal. For each such edge e , we introduce an arrow in $Q(G)$ connecting the faces separated by e ; this arrow is oriented so that when we move along the arrow in the direction

of its orientation, we see the white endpoint of e on our left and the black endpoint on our right. We then remove oriented 2-cycles from the resulting quiver, one by one, to get $Q(G)$. See Figure 7.5.

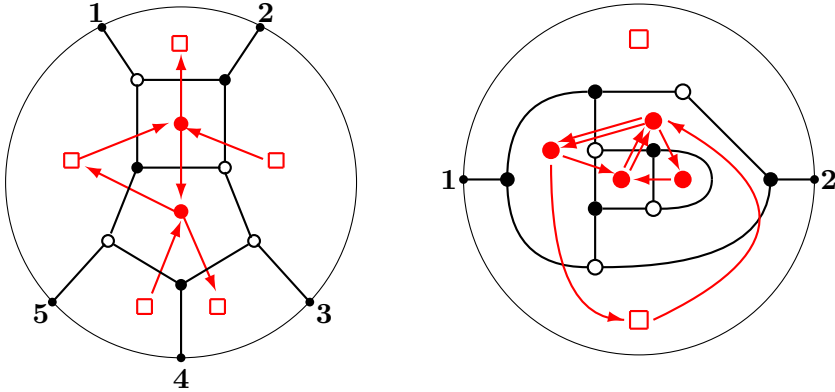


Figure 7.5. Two plabic graphs and their associated quivers. Shown on the left is the graph G from Figure 7.1(a). The quiver on the right has double arrows, corresponding to the instances where a pair of faces share two boundary segments disconnected from each other. The frozen vertex v at the top of the picture is isolated: the two arrows between v and an internal vertex located underneath v cancel each other.

Proposition 7.1.5. *Let G and G' be two plabic graphs related to each other by one of the local moves (M1), (M2), or (M3). Additionally, if G and G' are related via the square move (M1), then we require that*

(7.1.1) *among the four faces surrounding the square, the consecutive ones must be distinct, see Figure 7.6.*

Then the quivers $Q(G)$ and $Q(G')$ are mutation equivalent.

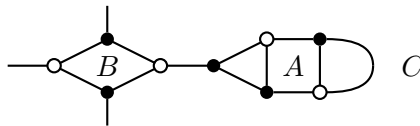


Figure 7.6. Restriction (7.1.1) allows the square move at A —but not at B , since face C is adjacent to two consecutive sides of B .

Proof. It is straightforward to check that a square move in a plabic graph translates into a quiver mutation at the vertex associated to that square face, provided that condition (7.1.1) is satisfied. It is also straightforward to check that the quiver associated with a plabic graph does not change under moves (M2) or (M3), see Figure 7.7. \square

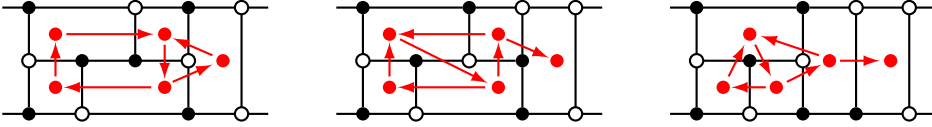


Figure 7.7. Fragments of plabic graphs and their associated quivers. The first two plabic graphs are related by a square move (M1); their quivers are related by a single mutation. The second and the third graphs are related by moves of type (M3), and have isomorphic quivers.

Remark 7.1.6. Suppose condition (7.1.1) fails at a square face B , with B incident to another face C along two consecutive edges, as in Figure 7.6. Then the arrows transversal to these edges cancel each other, so they do not appear in the associated quiver. This leads to a discrepancy between the square move and the quiver mutation.

Remark 7.1.7. The key difference between the setting of this section *vs.* Section 2.5 is that here we do not require plabic graphs to be bipartite. This distinction is not particularly important, since we can always apply a sequence of moves (M2) to a plabic graph to make it bipartite.

In the bipartite setting, the square move (M1) corresponds to urban renewal, see Definition 2.5.2 as well as Definition 7.5.13 below.

Remark 7.1.8. In light of Proposition 7.1.5, one may choose to adjust the definition of the square move (M1)—hence the notion of move equivalence of plabic graphs—by forbidding square moves violating condition (7.1.1). (This convention was adopted in [9].) We note that for the important subclass of *reduced* plabic graphs (see Definition 7.4.2 below), condition (7.1.1) is automatically satisfied, so there is no need to worry about it.

Remark 7.1.9. Using Definition 7.1.4, we can associate a seed pattern—hence a cluster algebra—to any plabic graph G . By Proposition 7.1.5, this cluster algebra only depends on the move equivalence class of G , assuming that we adopt a restricted notion of move equivalence, cf. Remark 7.1.8. We will soon see that this family of cluster algebras includes all the main examples of cluster algebras (defined by quivers) introduced in the earlier chapters. This justifies the importance of the combinatorial study of plabic graphs, and in particular their classification up to move equivalence.

The quivers arising from plabic graphs are rather special. In particular, each quiver $Q(G)$ is planar.

On the other hand, the mutation class of any quiver without frozen vertices can be embedded into the mutation class of a quiver of a plabic graph:

Proposition 7.1.10 ([8]). *Let Q be a quiver whose vertices are all mutable. Then there exists a plabic graph G such that Q is a full subquiver (see Definition 4.1.1) of a quiver mutation-equivalent to $Q(G)$.*

7.2. Triangulations and wiring diagrams via plabic graphs

In this section, we explain how the machinery of local moves on plabic graphs unifies the combinatorial constructions of Chapter 2, including:

- flips in triangulations of a polygon (Section 2.2);
- braid moves for wiring diagrams (Section 2.3);
- their analogues for double wiring diagrams (Section 2.4).

As mentioned in Remark 7.1.7, the urban renewal transformations (Section 2.5) can also be interpreted in terms of local moves in plabic graphs.

Example 7.2.1 (Triangulations of a polygon, see [16, Algorithm 12.1]). Let T be a triangulation of a convex m -gon \mathbf{P}_m . The plabic graph $G(T)$ associated to T is constructed as follows:

- (1) Place a white vertex of $G(T)$ at each vertex of \mathbf{P}_m .
- (2) Place a black vertex of $G(T)$ in the interior of each triangle of T . Connect it by edges to the three white vertices of the triangle.
- (3) Embed \mathbf{P}_m into the interior of a disk \mathbf{D} .
- (4) Place m uncolored vertices of $G(T)$ on the boundary of \mathbf{D} .
- (5) Connect each white vertex of $G(T)$ to a boundary vertex. These edges must not cross.

We emphasize that the set of edges of $G(T)$ includes neither the sides of \mathbf{P}_m nor the diagonals of T . See Figure 7.8.

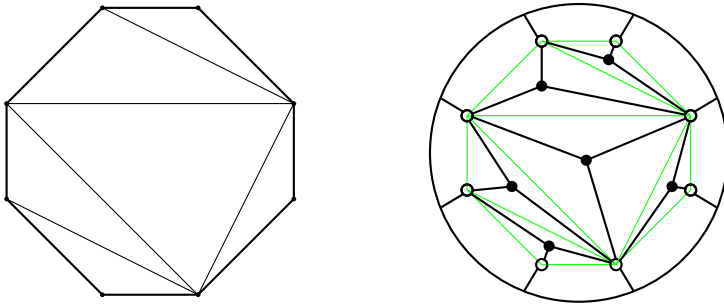


Figure 7.8. A triangulation T of an octagon, and the corresponding plabic graph $G(T)$, cf. Figure 2.2.

Exercise 7.2.2. Show that $Q(G(T)) = Q(T)$, i.e., the quiver associated to the plabic graph of a triangulation T coincides with the quiver $Q(T)$ associated to T , as in Definition 2.2.1.

Exercise 7.2.3. Show that if triangulations T and T' are related by a flip, then the plabic graphs $G(T)$ and $G(T')$ are move-equivalent to each other.

More concretely, flipping a diagonal in T translates into a square move at the corresponding quadrilateral face of $G(T)$, plus some (M3) moves to make each vertex of that face trivalent.

Example 7.2.4 (Wiring diagrams). Let D be a wiring diagram, as in Section 1.3. We associate a plabic graph $G(D)$ to D by replacing each crossing in D by a pair of trivalent vertices connected vertically, with a black vertex on top and a white vertex on the bottom. We then enclose the resulting graph in a disk.

This construction applies to a more general version of wiring diagrams. Let s_i denote the simple transposition in the symmetric group \mathcal{S}_n that exchanges i and $i + 1$. Given a sequence $\mathbf{w} = s_{i_1}s_{i_2}\dots s_{i_m}$ of simple transpositions, we associate to it a diagram $D(\mathbf{w})$ by concatenating m graphs; here the graph associated to s_j consists of n wires, of which $n - 2$ are horizontal, while the j th and $(j + 1)$ st wires cross over each other. See Figure 7.9.

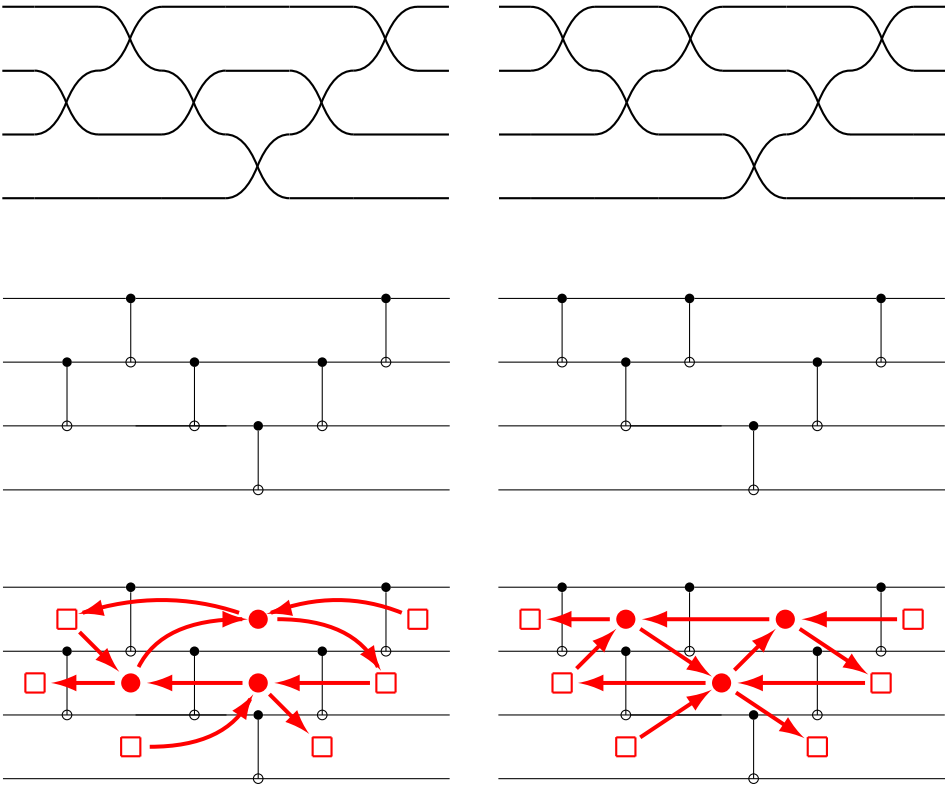


Figure 7.9. Top: the wiring diagrams D_1 and D_2 associated to reduced expressions $s_2s_3s_2s_1s_2s_3$ and $s_3s_2s_3s_1s_2s_3$ for $w_0 = (4, 3, 2, 1) \in S_4$. These wiring diagrams (resp., reduced expressions) are related via a braid move. Middle: the plabic graphs $G(D_1)$ and $G(D_2)$. Bottom: the quivers $Q(G(D_1))$ and $Q(G(D_2))$, with isolated frozen vertices removed.

Exercise 7.2.5. Show that after removing isolated frozen vertices at the top and bottom, the quiver $Q(G(D))$ associated to the plabic graph of a wiring diagram D coincides with the quiver $Q(D)$ associated to D , as in Definition 2.3.1, up to a global reversal of arrows.

Remark 7.2.6. If we changed our convention in Example 7.2.4, swapping the colors of the black and white vertices, we'd recover precisely the quiver $Q(D)$ associated to the wiring diagram. However, we prefer the convention used in Example 7.2.4 because it will lead to a transparent algorithm for recovering the chamber minors, as shown in Figure 7.62. And as noted in Remark 3.1.10, the cluster algebra associated to a given quiver is the same as the cluster algebra associated to the opposite quiver.

Remark 7.2.7. If two wiring diagrams D and D' are related by a braid move, then the corresponding plabic graphs $G(D)$ and $G(D')$ are related by a square move plus some (M3) moves, see Figure 7.10.

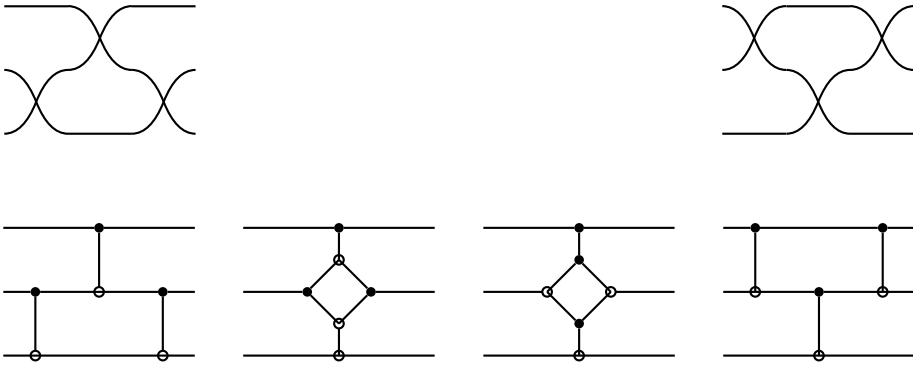


Figure 7.10. A braid move on wiring diagrams, and a corresponding sequence of moves on plabic graphs. The first two (resp., the last two) plabic graphs are related by two (M3) moves; the two plabic graphs in the middle are related by an (M1) move.

Example 7.2.8 (Double wiring diagrams). Let D be a double wiring diagram, as in Section 1.4. The plabic graph $G(D)$ associated to D is defined by adjusting the construction of Example 7.2.4 in the following way: as before, we replace each crossing in the double wiring diagram by a pair of trivalent vertices connected vertically, and color one of these vertices white and the other black. If the crossing is thin, the top vertex gets colored white and the bottom one black; if the crossing is thick, the colors of the two vertices are reversed. See Figure 7.11.

As in Example 7.2.4, the above construction works for a more general version of double wiring diagrams. Given two sequences $\mathbf{w} = s_{i_1} s_{i_2} \dots s_{i_m}$ and $\bar{\mathbf{w}} = \bar{s}_{j_1} \bar{s}_{j_2} \dots \bar{s}_{j_\ell}$, choose an arbitrary shuffle of \mathbf{w} and $\bar{\mathbf{w}}$. Then we can

associate a (generalized) double wiring diagram to this shuffle, where thick crossings are associated to factors in \mathbf{w} , and thin crossings are associated to factors in $\overline{\mathbf{w}}$. So, e.g., the double wiring diagram in Figure 7.11 is associated to the shuffle $\overline{s_2}s_1s_2\overline{s_1}\overline{s_2}s_1$.

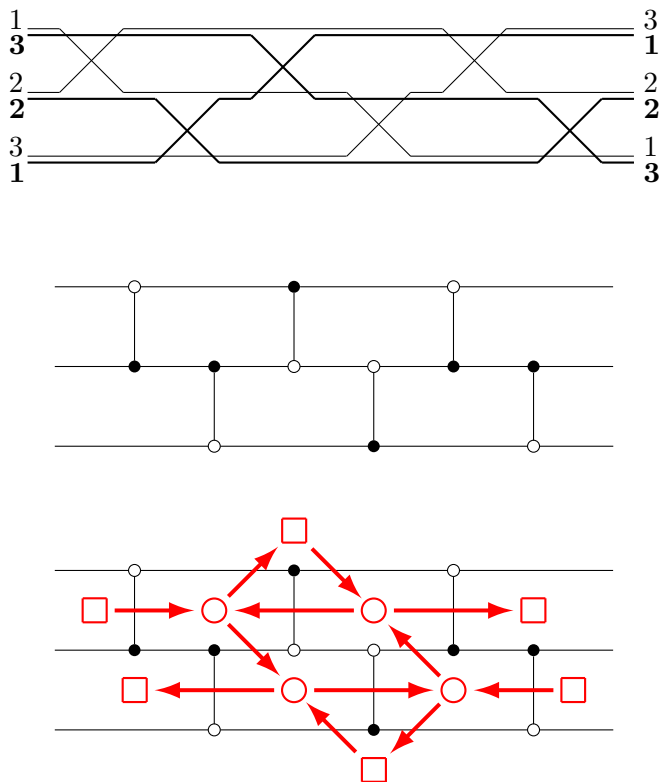


Figure 7.11. A double wiring diagram D , the corresponding plabic graph $G(D)$, and the quiver associated to $G(D)$. If one removes the bottom frozen vertex, one recovers the quiver from Figure 2.6 (up to a global reversal of arrows).

Exercise 7.2.9. Extend the statements of Exercise 7.2.5 and Remark 7.2.7 to the case of double wiring diagrams.

In addition to triangulations and (ordinary or double) wiring diagrams, plabic graphs can also be used to describe Fock-Goncharov cluster structures [7]:

Exercise 7.2.10. Construct a plabic graph whose associated quiver is the quiver shown in Figure 2.3. How does this construction generalize to a quiver $Q_3(T)$ associated to an arbitrary triangulation T of a convex polygon, cf. Exercise 2.2.3?

7.3. Trivalent plabic graphs

In Section 7.1, we introduced plabic graphs and described local moves that generate an equivalence relation on them. In this section, we focus on *trivalent plabic graphs*, i.e., those plabic graphs whose interior vertices are all trivalent. This will require working with an alternative set of moves that preserve the property of being trivalent.

Remark 7.3.1. Trivalent plabic graphs arise naturally in the studies of

- soliton solutions to the KP equation [16],
- sections of fine zonotopal tilings of 3-dimensional cyclic zonotopes [10],
- combinatorics of planar divides and associated links [9], and
- π -induced subdivisions for a projection π from the hypersimplex $\Delta_{k,n}$ to an n -gon [22].

We begin with the following simple observation.

Lemma 7.3.2. *Any plabic graph with no interior leaves (i.e., no degree 1 interior vertices) can be transformed by a sequence of moves of type (M2) and/or (M3) into a plabic graph all of whose interior vertices are trivalent.*

Proof. We can get rid of bivalent vertices using the moves (M2). If there are any vertices of degree ≥ 4 , split those vertices using (M3) until all internal vertices are trivalent. \square

The alternative set of moves for trivalent plabic graphs consists of the square move (M1) together with the *flip move* (M4) defined below.

Definition 7.3.3. The *flip move* (sometimes also called the *Whitehead move*) for trivalent plabic graphs is defined as follows:

(M4) Replace a fragment containing two trivalent vertices of the same color connected by an edge by another such fragment, see Figure 7.12.

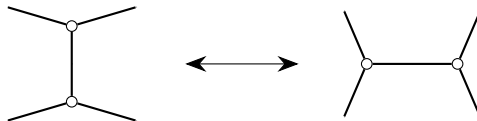


Figure 7.12. The flip move (or Whitehead move) for trivalent graphs. The four vertices shown should either all be white, or all be black.

Remark 7.3.4. A flip move (M4) can be expressed as a composition of two moves of type (M3).

The main result of this section is the following.

Theorem 7.3.5. *Two trivalent plabic graphs G and G' are related via a sequence of local moves of types (M1), (M2), and (M3) if and only if they are related by a sequence of moves of types (M1) and (M4).*

The rest of this section is devoted to the proof of Theorem 7.3.5.

Lemma 7.3.6. *If two trivalent plabic graphs G and G' are connected by a sequence of moves of type (M2) or (M3), then they are connected by a sequence of moves of type (M3).*

Proof. We first note that in many cases, move (M2) can be thought of as an instance of move (M3): instead of using (M2) to add or remove a bivalent vertex that is adjacent via an edge e to a vertex of the same color, we can use (M3) to (un)contract e , to the same effect.

The only (M2) moves that are genuinely different from (M3) moves are the (M2) moves that add or remove a white (resp., black) vertex in the middle of a black-black or black-boundary (resp., white-white or white-boundary) edge. We call them *creative* or *destructive* (M2) moves, see the left and middle of Figure 7.13. We need to show that it is never necessary to use a creative or destructive (M2) move to connect G and G' as above.

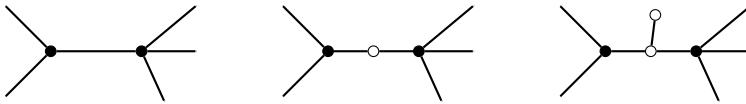


Figure 7.13. Using a creative (M2) move and then an (M3) move to grow a white leaf.

Consider a shortest sequence of (M2)/(M3) moves connecting G and G' :

$$(7.3.1) \quad G = G_0 \sim G_1 \sim \cdots \sim G_k = G'.$$

We first claim that each G_i does not contain an internal leaf. Suppose otherwise. Let $G_{i-1} \sim G_i$ be the last step when we grow a leaf (as in Figure 7.13). That is, i is maximal such that G_i has a leaf v' attached via edge e to some vertex v , where v' and e were not present in G_{i-1} . Since G' has no leaves, there must be some $j > i$ such that G_j is obtained from G_{j-1} by contracting the edge adjacent to v' . By construction, each graph $G_i, G_{i+1}, \dots, G_{j-1}$ contains leaf v' along with a path connecting v' to a vertex of the same color; this path is obtained by subdividing the edge e by adding bivalent vertices (which must remain bivalent since no new leaves may be added). But then we can construct a shorter sequence of moves connecting G to G' by removing all steps used to create and contract this path.

Having established that none of the graphs appearing on the shortest path (7.3.1) have internal leaves, we will now demonstrate that this path never uses a creative or destructive (M2) move. Note that we cannot have only destructive (M2) moves because (M3) moves alone cannot create a vertex whose removal requires a destructive (M2) move. Thus, it is enough to show that we cannot have a creative (M2) move along (7.3.1). Suppose there is one, and that the last creative (M2) move adds a bivalent white vertex w along a black-black edge. Along (7.3.1), this bivalent vertex w might split into multiple bivalent white vertices (pairwise adjacent, in a row). However, all these vertices must get removed somewhere along (7.3.1), since G' has no bivalent vertices. We can then shorten (7.3.1) by removing all moves involving these bivalent vertices. The lemma is proved. \square

Lemma 7.3.7. *Let G and G' be two trivalent plabic graphs such that*

- *each of the graphs G and G' is connected;*
- *each of the graphs G and G' has f interior faces, b boundary vertices, and b boundary faces (the number of boundary vertices equals the number of boundary faces since the graphs are connected);*
- *in each of the graphs G and G' , all interior vertices have the same color, and this color is the same in both graphs.*

Then G and G' can be connected by a sequence of flip moves (M4).

Proof. The *dual graph* G_{dual} of a trivalent connected plabic graph G is obtained as follows. Place a vertex of G_{dual} in the interior of each face of G . For each edge e of G , introduce a (transversal) edge of G_{dual} connecting the vertices of G_{dual} located in the faces of G on both sides of e , see Figure 7.14. (This new edge may be a loop.) Under the conditions of the lemma, the dual graph G_{dual} is a generalized triangulation T of a (dual) b -gon. (We note that T may contain *self-folded* triangles – loops with an interior “pendant” edge – coming from the faces of G enclosed by a loop in G , as in Figure 7.14.) The triangulation T has $b + f$ vertices: the b vertices of the dual b -gon together with the f interior points (“punctures”).

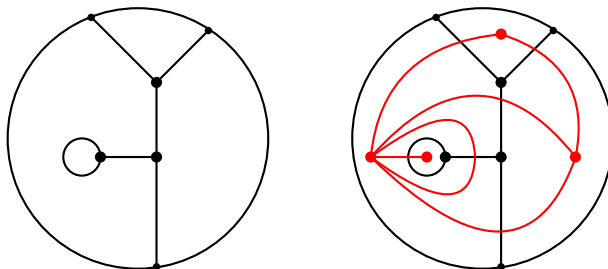


Figure 7.14. A trivalent plabic graph G and its dual graph G_{dual} (in red); the latter contains a self-folded triangle. Here $b = 3$ and $f = 1$.

Figure 7.15 shows that a flip move in a trivalent plabic graph corresponds to a flip in the corresponding triangulation. The claim that G and G' are connected by flip moves can now be obtained from the well-known fact [11, 12] that any two triangulations of a b -gon with f interior points are connected by flips. \square

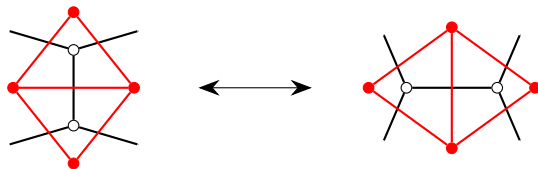


Figure 7.15. The flip move for trivalent graphs corresponds to a flip of the corresponding dual triangulations.

Definition 7.3.8. A *white component* W of a plabic graph G is obtained by taking a maximal (by inclusion) connected induced subgraph of G all of whose internal vertices are white, together with the half-edges extending from the (white) vertices of W towards black vertices outside W or towards boundary vertices of G . *Black components* of G are defined in the same way, with the roles of black and white vertices reversed.

Remark 7.3.9. Each black or white component C of a plabic graph G can itself be regarded as a (generalized) plabic graph. To this end, enclose C by a simple closed curve γ passing through the endpoints of the half-edges on the outer boundary of C . If the portion of G located inside γ is exactly C , then we get a usual plabic graph. It may however happen that C contains “holes,” i.e., some of the half-edges on the boundary of C may be entirely contained in the interior of the disk enclosed by γ . In that case, we need to draw simple closed curves through the endpoints of those half-edges, so that C becomes a generalized plabic graph inside a “swiss-cheese” shape (a disk with some smaller disks removed), as in Figure 7.16. The argument in the proof of Lemma 7.3.7 extends to this setting, so Lemma 7.3.7 also holds for black/white components of trivalent plabic graphs. We will use this generalization in the proof of Proposition 7.3.10 below.

Proposition 7.3.10. *Let two trivalent plabic graphs be related to each other by moves (M2) or (M3). Then they are related by a series of flip moves (M4).*

Proof. Let G and G' be the plabic graphs in question. Without loss of generality we may assume that G and G' are connected. By Lemma 7.3.6, G and G' are connected by moves (M3).

Each of the graphs G and G' breaks into disjoint (white or black) components. Each (M3) move only affects a single component. It follows that the white (resp., black) components W_1, \dots, W_ℓ (resp., B_1, \dots, B_m) of G

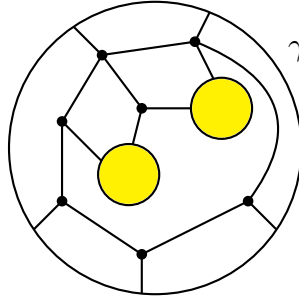


Figure 7.16. A generalized plabic graph inside a “swiss-cheese” shape (in this case, a disk with two smaller disks removed).

are in bijection with the components W'_1, \dots, W'_ℓ (resp., B'_1, \dots, B'_m) of G' , so that each W_i (resp., B_j) is related to W'_i (resp., B'_j) via (M3) moves.

Since an (M3) move preserves both the number of boundary vertices and the number of faces of a graph, both W_i and W'_i (respectively, B_j and B'_j) have the same number of boundary vertices and the same number of faces. It now follows from Lemma 7.3.7 (more precisely, from its extension to components of plabic graphs, see Remark 7.3.9) that each pair W_i and W'_i can be connected by flip moves, and similarly for B_j and B'_j . The proposition follows. \square

Proof of Theorem 7.3.5. The “if” direction immediately follows from Remark 7.3.4.

Suppose that G and G' are related via a sequence of (M1), (M2), and (M3) moves. Let k denote the number of square moves (M1) in the sequence. We then have a sequence of move-equivalences

$$G = G'_0 \sim G_1 \sim G'_1 \sim G_2 \sim G'_2 \sim \dots \sim G_k \sim G'_k \sim G_{k+1} = G',$$

where for all i ,

- G_i is related to G'_i by a single square move;
- G'_i is related to G_{i+1} by a sequence of (M2) and (M3) moves.

Since a square move only involves trivalent vertices, we may assume, applying extra (M2) and (M3) moves as needed, that all plabic graphs G_i and G'_i are trivalent. It then follows by Proposition 7.3.10 that for every i , the graphs G'_i and G_{i+1} are related by flip moves alone, and we are done. \square

Remark 7.3.11. The plabic graphs associated to wiring diagrams and double wiring diagrams as in Example 7.2.4 and Example 7.2.8 are trivalent, and consequently one can express the transformation corresponding to braid moves using square moves and flip moves, as shown in Figure 7.10.

On the other hand, the plabic graphs associated to triangulations of a polygon (see Example 7.2.1 and Figure 7.8) are *not* trivalent.

7.4. Trips. Reduced plabic graphs

Reduced plabic graphs are a subclass of plabic graphs that play a critically important role in the study of cluster structures and total positivity in Grassmannians. In this section, we introduce reduced plabic graphs and various related concepts. The main result of the section, Theorem 7.4.25, provides a criterion for move equivalence of reduced plabic graphs. The proof of this theorem will occupy Sections 7.5–7.7.

Definition 7.4.1. We say that T is a *collapsible tree* in a plabic graph G if

- T is a tree with at least one edge not incident to the boundary of G ;
- T is an induced subgraph of G ;
- T is attached to the rest of G at a single vertex v , the *root* of T , so that
 - if v is a boundary vertex, one can use local moves (M2)–(M3) to collapse T to a lollipop based at v .
 - if v is an internal vertex, one can use local moves (M2)–(M3) to collapse T onto the vertex v .

In other words, local moves can be used to replace the tree T by either a lollipop based at v , or by v . See Figure 7.17.

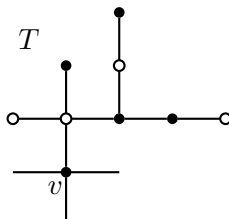


Figure 7.17. A collapsible tree T whose root is the internal vertex v .

Definition 7.4.2. A plabic graph G is *reduced* if no plabic graph $G' \sim G$ contains one of the following “forbidden configurations:”

- a *hollow digon*, i.e., two edges connecting a pair of distinct vertices, with no other edges in the region between them; or
- an internal leaf that is not a lollipop and does not belong to a collapsible tree.

See Figure 7.18 for a slightly modified (but equivalent) version.

Remark 7.4.3. For plabic graphs, the property of being reduced is, by definition, invariant under local moves.

Remark 7.4.4. As stated, this property is not readily testable, because the move equivalence class of a plabic graph is usually infinite. We will later obtain criteria (see Theorems 7.8.6 and 7.11.5) for testing this property.

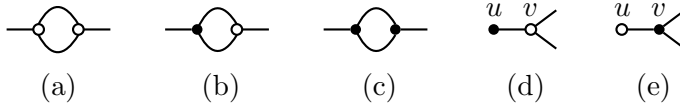


Figure 7.18. A plabic graph is not reduced if and only if it is move-equivalent to a graph containing a hollow digon, as in (a,b,c), or a graph containing an internal leaf u adjacent to a trivalent vertex v of opposite color such that v is not a root of a collapsible tree, see (d,e).

Remark 7.4.5. The notion of a reduced plabic graph, as introduced above in Definition 7.4.2, may appear artificial, as the choice of forbidden configurations is not well motivated. We will soon present alternative definitions of reducedness (in slightly restricted generality) that are both more conceptual and more elegant; see Proposition 7.4.9 and Corollary 7.4.26. In particular, these alternative definitions do not involve the forbidden configurations in Figure 7.18(d,e).

Remark 7.4.6. The requirement in Figure 7.18(d,e) concerning the collapsible tree cannot be removed: as shown in Figure 7.19, dropping this requirement would make *any* plabic graph non-reduced.

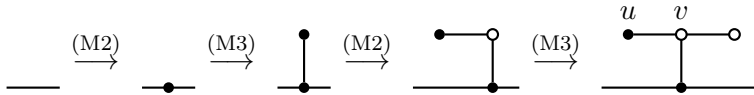


Figure 7.19. Any plabic graph can be transformed via moves (M2)–(M3) into a graph containing a configuration as in Figure 7.18(d,e) in which vertex v is the root of a collapsible tree that contains vertex u .

Reduced plabic graphs can be interpreted as generalizations of reduced expressions in symmetric groups:

Exercise 7.4.7. Consider sequences (or “words”) $\mathbf{w} = s_{i_1} \cdots s_{i_m}$ of simple transpositions in a symmetric group, as in Example 7.2.4. We say that two such words are *braid-equivalent* if they can be related to each other using the braid relations $s_i s_{i+1} s_i = s_{i+1} s_i s_{i+1}$ and $s_i s_j = s_j s_i$ for $|i - j| \geq 2$. A word \mathbf{w} is called a *reduced expression* if no word in its braid equivalence class has two consecutive equal entries: $\cdots s_i s_i \cdots$. Show that if \mathbf{w} fails to be a reduced expression, then $G(D(\mathbf{w}))$ fails to be a reduced plabic graph.

Remark 7.4.8. Conversely, if \mathbf{w} is reduced, then $G(D(\mathbf{w}))$ is reduced; this can be proved using Theorem 7.8.6 or Theorem 7.11.5.

Proposition 7.4.9. *Let G be a plabic graph that has no internal leaves, other than lollipops. Then the following are equivalent:*

- (i) G is not reduced;
- (ii) G can be transformed, via local moves that do not create internal leaves, into a plabic graph containing a hollow digon, cf. Figure 7.18(a,b,c).

We note that in the absence of internal leaves, the only forbidden configurations are the hollow digons.

The proof of Proposition 7.4.9 will require some technical preparations, see Definition 7.4.10 and Lemma 7.4.11 below.

Definition 7.4.10. We denote by \overline{G} the plabic graph obtained from G by repeatedly collapsing all collapsible trees. It is not hard to see that \overline{G} is uniquely defined.

Lemma 7.4.11. *Let G be a plabic graph such that \overline{G} has no internal leaves, other than lollipops. Let G' be a plabic graph obtained from G by a local move. Assume that this move is not a square move (M1) where one of the vertices of the square (in G) is the root of a collapsible tree. Then $\overline{G'}$ has no internal leaves, other than lollipops. Moreover, \overline{G} and $\overline{G'}$ are either equal to each other or related by a single local move.*

Proof. If the changes resulting from the local move $G \rightarrow G'$ occur within a collapsible tree, then the tree remains collapsible, so $\overline{G'} = \overline{G}$. Otherwise, the same move can be applied in \overline{G} , yielding $\overline{G'}$ (and not creating any leaves). \square

Proof of Proposition 7.4.9. The implication (ii) \Rightarrow (i) is immediate. Let us establish (i) \Rightarrow (ii). Assume that G is not reduced. Then there exists a sequence of plabic graphs

$$(7.4.1) \quad G = G_0, G_1, \dots, G_N$$

in which each pair (G_i, G_{i+1}) is related by a local move and moreover G_N contains a forbidden configuration from Figure 7.18.

Case 1: the sequence (7.4.1) does not include a square move $G_k \xrightarrow{(M1)} G_{k+1}$ where one of the vertices of the square in G_k is the root of a collapsible tree. Repeatedly applying Lemma 7.4.11, we conclude that the graphs $\overline{G_i}$ do not contain internal leaves, other than lollipops. Moreover, for each i , the plabic graphs $\overline{G_i}$ and $\overline{G_{i+1}}$ either coincide or are related via a single local move. It is furthermore easy to see that since G_N contains a forbidden configuration, then the same must be true for $\overline{G_N}$. That is, $\overline{G_N}$ contains a hollow digon. We conclude that $G = G_0 = \overline{G_0}$ is connected by local moves that do not create internal leaves to a plabic graph $\overline{G_N}$ containing a hollow digon.

Case 2: the sequence (7.4.1) includes a square move $G_k \xrightarrow{(M1)} G_{k+1}$ in which one of the vertices of the square in G_k is the root of a collapsible tree. Let (G_k, G_{k+1}) be the first such occurrence (i.e., the one with the smallest k). Repeatedly applying Lemma 7.4.11, we conclude that $G = \overline{G_0}$ is related to $\overline{G_k}$ via local moves that do not create internal leaves. Moreover, $\overline{G_k}$ contains

a square configuration in which one of the vertices of the square is bivalent. Removing this vertex using (M2) and contracting the resulting edge yields a bicolored hollow digon, and we are done. \square

The most fundamental result concerning reduced plabic graphs is their classification up to move equivalence (cf. Remark 7.4.3), to be given in Theorem 7.4.25 below. To state this result, we will need some preparation.

Definition 7.4.12. A *trip* τ in a plabic graph G is a directed walk along the edges of G that either begins and ends at boundary vertices (with all intermediate vertices internal), or is a closed walk entirely contained in the interior of the disk, which obeys the following *rules of the road*:

- at a black vertex, τ always makes the sharpest possible right turn;
- at a white vertex, τ always makes the sharpest possible left turn.

If the trip begins and ends at boundary vertices we call it a *one-way trip*; if it is a closed walk entirely contained in the interior of the disk, we call it a *roundtrip*.

The endpoints of a one-way trip may coincide with each other. For example, the trip corresponding to a lollipop rooted at a vertex i starts and ends at i .

Remark 7.4.13. Just as different countries have different rules regarding which side of the road one should drive on, different authors make conflicting choices for the rules of the road for plabic graphs. In this book, we consistently use the convention chosen in Definition 7.4.12.

Remark 7.4.14. The notion of a trip and the condition of being reduced have appeared in the study of dimer models in statistical mechanics, wherein trips have been called *zigzag paths* [14]. Reduced plabic graphs were called “marginally geometrically consistent” in [4, Section 3.4], and were said to “obey condition Z” in [3, Section 8].

Remark 7.4.15. For any edge e in G , there is a unique trip traversing e in each of the two directions. It may happen that the same trip traverses e twice (once in each direction).

Exercise 7.4.16. Show that one-way trips starting at different vertices terminate at different vertices.

Exercise 7.4.17. Let $G(D)$ be a plabic graph associated to some wiring diagram D , see Example 7.2.4 and Figure 7.9. Show that the trips starting at the left side of $G(D)$ follow the pattern determined by the strands of D , while the trips starting at the right side of $G(D)$ proceed horizontally to the left. Describe the trips in a plabic graph associated to a double wiring diagram.

Definition 7.4.18. Let G be a plabic graph with b boundary vertices. The *trip permutation* $\pi_G : \{1, \dots, b\} \rightarrow \{1, \dots, b\}$ is defined by setting $\pi_G(i) = j$ whenever the trip originating at i terminates at j . We will mostly use the one-line notation $\pi_G = (\pi_G(1), \dots, \pi_G(b))$ to represent these permutations.

To illustrate, in Figure 7.1(a), we have $\pi_G = (3, 4, 5, 1, 2)$.

Exercise 7.4.19. Show that move-equivalent plabic graphs have the same trip permutation.

The notion of a trip permutation can be further enhanced to construct finer invariants of local moves. For example, we can record, in addition to the trip permutation, the suitably defined *winding number* of each trip. These winding numbers do not change under local moves (with one subtle exception, cf. Figure 7.34 below). A more powerful invariant associates to any plabic graph a particular (transverse) link, see [9].

Definition 7.4.20. A *decorated permutation* $\tilde{\pi}$ on b letters is a permutation of the set $\{1, \dots, b\}$ together with a *decoration* of each fixed point by either an overline or an underline. In other words, for every i , we have

$$\tilde{\pi}(i) \in \{\bar{i}, \underline{i}\} \cup \{1, \dots, b\} \setminus \{i\}.$$

An example of a decorated permutation on 6 letters is $(3, 4, 5, 1, 2, \bar{6})$.

Exercise 7.4.21. Show that the number of decorated permutations on b letters is equal to $b! \sum_{k=0}^b \frac{1}{k!}$.

The following statement will be proved in Section 7.7.

Proposition 7.4.22. *Let G be a reduced plabic graph. If $\pi_G(i) = i$, then the connected component of G containing the boundary vertex i collapses to a lollipop.*

In Proposition 7.4.22, the requirement that G is reduced cannot be dropped, see Figure 7.20.

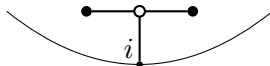


Figure 7.20. A non-reduced plabic graph G with $\pi_G(i) = i$, cf. Figure 7.18(d). The component containing i is not collapsible.

Definition 7.4.23. Let G be a reduced plabic graph with b boundary vertices. The *decorated trip permutation* associated with G is defined as follows:

$$\tilde{\pi}_G(i) = \begin{cases} \pi_G(i) & \text{if } \pi_G(i) \neq i; \\ \bar{i} & \text{if } G \text{ contains a tree collapsing to a white lollipop at } i; \\ \underline{i} & \text{if } G \text{ contains a tree collapsing to a black lollipop at } i. \end{cases}$$

Figure 7.21 shows two reduced plabic graphs with the same decorated trip permutation $(3, 4, 5, 1, 2, \bar{6})$.

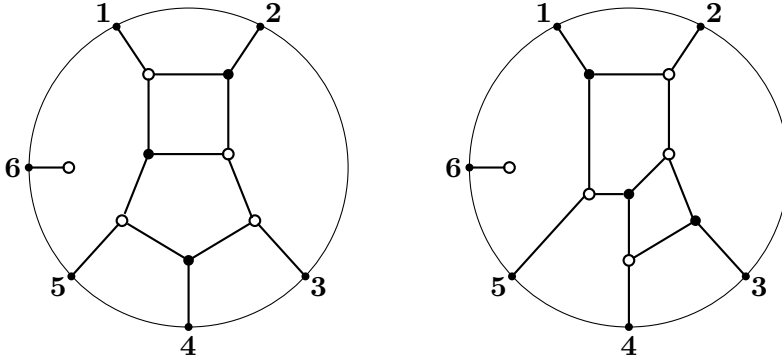


Figure 7.21. Two reduced plabic graphs sharing the same decorated trip permutation $(3, 4, 5, 1, 2, \bar{6})$. Cf. Figure 7.1(b).

Exercise 7.4.19 can be strengthened as follows.

Exercise 7.4.24. The decorated trip permutation of a reduced plabic graph is invariant under local moves.

We will later show (see Corollary 7.10.4) that for each decorated permutation $\tilde{\pi}$ on b letters, there exists a reduced plabic graph whose decorated trip permutation is $\tilde{\pi}$.

Crucially, the move-equivalence class of a reduced plabic graph is completely determined by its decorated trip permutation:

Theorem 7.4.25 (Fundamental theorem of reduced plabic graphs). *Let G and G' be reduced plabic graphs. The following statements are equivalent:*

- (1) G and G' are move-equivalent;
- (2) G and G' have the same decorated trip permutation.

To illustrate, the two reduced plabic graphs shown in Figure 7.21 have the same decorated trip permutation and consequently are move-equivalent.

The statement (1) \Rightarrow (2) in Theorem 7.4.25 is easy, cf. Exercise 7.4.24. The converse implication (2) \Rightarrow (1) is much harder. In Section 7.7, we give a proof of this implication that utilizes D. Thurston's machinery of triple diagrams, which is presented in Sections 7.5–7.6.

A very intricate argument justifying the implication (2) \Rightarrow (1) was given in A. Postnikov's original preprint [21, Section 13]. Another proof of Theorem 7.4.25, involving some difficult results about *plabic tilings* (and relying on Theorem 7.13.4 below), was given by S. Oh and D. Speyer [20].

Corollary 7.4.26. *Let π be a permutation on b letters. Consider all plabic graphs G without internal leaves (other than lollipops) whose trip permutation is π ; in particular, G has b boundary vertices. Among all such plabic graphs G , the reduced ones are precisely those that have the smallest number of faces.*

Proof. Local moves do not change the number of faces. It follows by Theorem 7.4.25 that all reduced plabic graphs with a given decorated trip permutation have the same number of faces.

Changing the color of a lollipop transforms a reduced plabic graph into another reduced graph with the same number of faces and the same trip permutation (but with different decoration). Therefore all reduced plabic graphs G with $\pi(G) = \pi$ have the same number of faces.

It remains to show that if G is not reduced and has no internal leaves other than lollipops, then there exists a plabic graph G' with $\pi(G') = \pi$ and with fewer faces than G . We note that under our assumptions on G , Proposition 7.4.9 applies, so G can be transformed by local moves that do not create internal leaves into a plabic graph G'' containing a hollow digon. We now claim that G'' can be replaced by a plabic graph G''' (not move-equivalent to G'') such that G'' and G''' have the same trip permutation but G''' has fewer faces than G'' . The recipe for constructing G''' is as follows. If the vertices of the hollow digon in G'' are of the same color, then remove one of the sides of the digon (keeping its vertices) to get G''' . If, on the other hand, the vertices of the digon have different colors, then remove both sides of the digon; if one of the vertices was bivalent, then remove it as well. It is straightforward to check that in each case, the trip permutation does not change whereas the number of faces decreases by 1 or 2. \square

In Corollary 7.10.5, we will give a formula for the number of faces in a reduced plabic graph in terms of the associated decorated trip permutation.

Remark 7.4.27. In Corollary 7.4.26, the requirement that G has no internal leaves cannot be dropped. For example, the graph in Figure 7.20 has a single face but is not reduced.

Remark 7.4.28. Some authors call a plabic graph reduced if it has the smallest number of faces among all graphs with a given decorated trip permutation, cf. Corollary 7.4.26. If one adopts this definition, then the graph G in Figure 7.20 becomes reduced. This leads to a failure of Proposition 7.4.22, since the component of G attached to the boundary vertex i does not collapse to a lollipop.

Another reason to treat this kind of plabic graph G as non-reduced will arise in the context of triple diagrams, cf. Section 7.7. While reduced plabic graphs should correspond to minimal triple diagrams (see Theorem 7.7.3), the triple diagram corresponding to G is not minimal.

7.5. Triple diagrams and normal plabic graphs

Triple diagrams (or triple crossing diagrams), introduced by D. Thurston in [24], are planar topological gadgets closely related to plabic graphs. Our treatment of triple diagrams in Sections 7.5–7.6 is largely based on [24].

Definition 7.5.1. Consider a collection \mathfrak{X} of oriented intervals and/or circles immersed into a disk \mathbf{D} . Their images are collectively called *strands*. The images of immersed intervals (resp., circles) are the *arcs* (resp., *closed strands*) of \mathfrak{X} . A *face* of \mathfrak{X} is a connected component of the complement of the union of the strands within \mathbf{D} . We call \mathfrak{X} a *triple diagram* if

- the preimage of each point in \mathbf{D} consists of either 0, 1, or 3 points; in the latter case of a *triple point*, the three local branches intersect transversally in the interior of \mathbf{D} ;
- the endpoints of arcs are distinct points located on the boundary $\partial\mathbf{D}$; each arc meets the boundary transversally;
- the union of the strands and the boundary of the disk is connected; this ensures that each face is homeomorphic to an open disk;
- the strand segments lying on the boundary of each face are oriented consistently (i.e., clockwise or counterclockwise); in particular, as we move along the boundary, the *sources* (endpoints where an arc runs away from $\partial\mathbf{D}$) alternate with the *targets* (where an arc runs into $\partial\mathbf{D}$).

Each triple diagram, say with b arcs, comes with a selection of b points on $\partial\mathbf{D}$ (called *boundary vertices*) labeled $1, \dots, b$ in clockwise order. There is one such boundary vertex within every other segment of $\partial\mathbf{D}$ between two consecutive arc endpoints. Specifically, we place boundary vertices so that, moving clockwise along the boundary, each boundary vertex follows (resp., precedes) a source (resp., a target). See Figure 7.22.

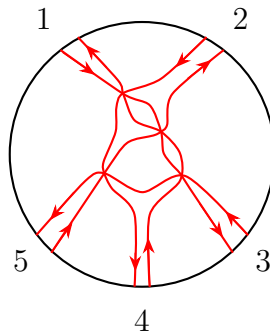


Figure 7.22. A triple diagram \mathfrak{X} with the strand permutation $\pi_{\mathfrak{X}} = (3, 4, 5, 1, 2)$.

Triple diagrams are considered up to smooth isotopy among such diagrams. This makes them essentially combinatorial objects: 6-valent/univalent directed graphs with some additional structure.

Remark 7.5.2. In [24], the definition of a triple diagram does not include the restriction appearing in Definition 7.5.1 that requires the union of the strands and the boundary $\partial\mathbf{D}$ to be connected. In the terminology of [24], all our triple diagrams are *connected*.

Remark 7.5.3. In order to ensure consistent orientations along the face boundaries, the orientations of strands must alternate between “in” and “out” around each triple point. Given a triple diagram with unoriented strands, we can satisfy this condition as follows: start anywhere and propagate out by assigning alternating orientations around vertices.

Definition 7.5.4. Let \mathfrak{X} be a triple diagram with b boundary vertices (hence b arcs). For each boundary vertex i , let s_i (resp., t_i) denote the source (resp., target) arc endpoint located next to i on the boundary of \mathbf{D} .

The *strand permutation* $\pi_{\mathfrak{X}}$ is defined by setting $\pi_{\mathfrak{X}}(i) = j$ whenever the arc originating at s_i ends up at t_j . Thus, the strand permutation describes the connectivity of the arcs. See Figure 7.22.

We will soon see (cf. Definition 7.6.8 below) that any permutation can arise as a strand permutation of a triple diagram.

Just as the local moves on plabic graphs preserve the (decorated) trip permutation (see Exercise 7.4.24), there is a notion of a local move on triple diagrams that keeps the strand permutation invariant.

Definition 7.5.5. We say that two triple diagrams \mathfrak{X} and \mathfrak{X}' are *move-equivalent* to each other, and write $\mathfrak{X} \sim \mathfrak{X}'$, if one can get between \mathfrak{X} and \mathfrak{X}' via a sequence of *swivel moves* shown in Figure 7.23. (These moves are called $2 \leftrightarrow 2$ moves in [24].)

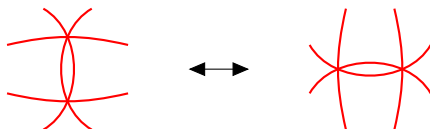


Figure 7.23. The swivel move replaces one of these fragments of a triple diagram by the other fragment, then smooths out the strands. The orientation of each strand on the left should match the orientation of the strand on the right that has the same endpoints.

Remark 7.5.6. The connectivity of strands on both sides of Figure 7.23 is the same, so the strand permutation is invariant under the swivel move.

We will soon see that triple diagrams are essentially cryptomorphic to plabic graphs—or more precisely, to the subclass of normal plabic graphs defined below.

Definition 7.5.7. We say that a plabic graph G is *normal* if the coloring of its internal vertices is bipartite, all white vertices in G are trivalent, and each boundary vertex is adjacent to a black vertex. See Figure 7.24.

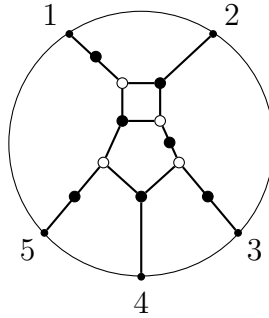


Figure 7.24. A normal plabic graph G . This graph was obtained from the one in Figure 7.1(a) by inserting several bivalent black vertices.

Remark 7.5.8. Since a normal plabic graph does not have white leaves, it cannot contain a tree that collapses to a white lollipop. Therefore, in the case of normal graphs, there is no need to decorate the trip permutation.

Definition 7.5.9. The triple diagram $\mathfrak{X}(G)$ associated to a normal plabic graph G is constructed as follows. To each trip in G —either a one-way trip or a roundtrip—we associate a strand in the ambient disk \mathbf{D} by slightly deforming the trip, as shown in Figure 7.25, so that the strand

- runs along each edge of the trip, keeping the edge on its left,
- makes a U-turn at each black internal leaf (a vertex of degree 1);
- ignores black vertices of degree 2,
- makes a right turn (as sharp as possible) at each other black vertex, and
- makes a left turn at each white vertex v along the trip, passing through v .

This collection of strands forms a triple diagram $\mathfrak{X}(G)$, see Figure 7.26 and Lemma 7.5.10.

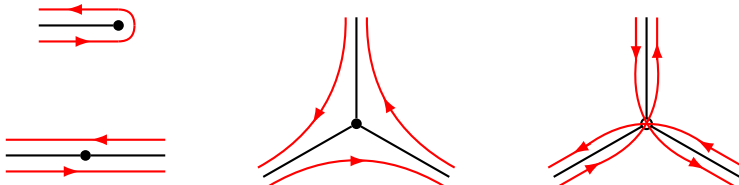


Figure 7.25. Constructing a triple diagram from a normal plabic graph.

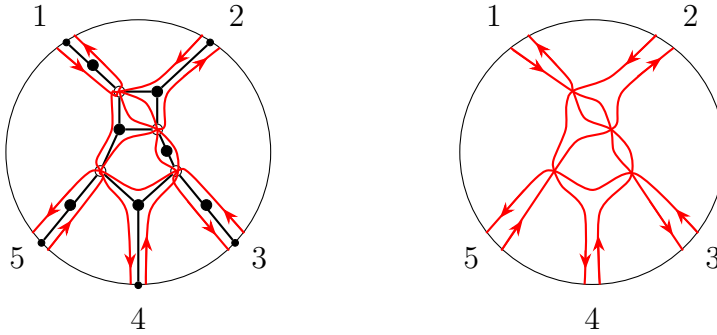


Figure 7.26. Left: A normal plabic graph G (cf. Figure 7.24) together with the associated triple diagram $\mathfrak{X} = \mathfrak{X}(G)$. Conversely, $G = G(\mathfrak{X})$. Right: The triple diagram $\mathfrak{X} = \mathfrak{X}(G)$. The trip permutation of G and the strand permutation of \mathfrak{X} are equal: $\pi_G = \pi_{\mathfrak{X}} = (3, 4, 5, 1, 2)$.

Lemma 7.5.10. *The diagram $\mathfrak{X}(G)$ associated to a normal plabic graph G as in Definition 7.5.9 is a triple diagram.*

Proof. Since the white vertices in G are trivalent, $\mathfrak{X}(G)$ has a triple point for every white vertex in G , and no other crossings. We need to check that $\mathfrak{X} = \mathfrak{X}(G)$ is connected, or more precisely, that the union of the strands and the boundary of the disk is connected, as required by Definition 7.5.1.

Let us ignore any component consisting of a single black vertex which is adjacent only to boundary vertices (e.g. a black lollipop), as the corresponding strands are clearly connected to the boundary of the disk. Consider any other strand S in \mathfrak{X} . By construction, S passes through at least one white vertex of the (bipartite) graph G , which is a triple point on S . It therefore suffices to show that every triple point in \mathfrak{X} is connected to the boundary within \mathfrak{X} (i.e., via strand segments of \mathfrak{X}).

Let u be a k -valent black vertex in G and let v_1, \dots, v_k be the white or boundary vertices adjacent to u . The strands of \mathfrak{X} that run along the k edges of G incident to u cyclically connect the triple points v_1, \dots, v_k to each other. (If the list v_1, \dots, v_k includes boundary vertices, then the corresponding strand segments are connected via the boundary.) We conclude that for any two-edge path $v - u - v'$ in G connecting two white or boundary vertices v and v' via a black vertex u , the triple (or nearby boundary) points v and v' are connected within \mathfrak{X} . It follows that for any path in the bipartite graph G connecting a white vertex v to the boundary, there is a path in \mathfrak{X} that connects the triple point v to the boundary.

It remains to note that by Definition 7.1.1, any white vertex v in G is connected by a path in G to some boundary vertex. \square

We now go in the opposite direction, from a triple diagram to a normal plabic graph.

Definition 7.5.11. The normal plabic graph $G = G(\mathfrak{X})$ associated to a triple diagram \mathfrak{X} is constructed as follows. Place a white vertex of G at each triple crossing in \mathfrak{X} . Treat each boundary vertex of \mathfrak{X} as a boundary vertex of G . For each region R of \mathfrak{X} whose boundary is oriented counterclockwise, place a black vertex in the interior of R and connect it to the white and boundary vertices lying on the boundary of R , so that each white (resp., boundary) vertex is trivalent (resp., univalent). The resulting plabic graph $G = G(\mathfrak{X})$ is normal by construction.

Proposition 7.5.12. *The maps $G \mapsto \mathfrak{X}(G)$ and $\mathfrak{X} \mapsto G(\mathfrak{X})$ described in Definitions 7.5.9 and 7.5.11 are mutually inverse bijections between normal plabic graphs and triple diagrams with the same number of boundary vertices. The trip permutation π_G of a normal graph G is equal to the strand permutation $\pi_{\mathfrak{X}}$ of the corresponding triple diagram $\mathfrak{X} = \mathfrak{X}(G)$.*

Proof. Starting from a normal graph G , let us decompose it into star-shaped subgraphs S_v each of which includes a black vertex v , all the edges incident to v , and the endpoints of those edges. Each of these stars will give rise to a fragment of the triple diagram $\mathfrak{X}(G)$ that “hugs” the edges of S_v and whose boundary is oriented counterclockwise (looking from S_v). Moreover, $\mathfrak{X}(G)$ is obtained by stitching these fragments together. Applying the map $\mathfrak{X} \mapsto G(\mathfrak{X})$ to $\mathfrak{X}(G)$ will recover the original graph G .

One similarly shows that if we start from a triple diagram \mathfrak{X} , construct the normal graph $G(\mathfrak{X})$, and then apply the map $G \mapsto \mathfrak{X}(G)$ to $G(\mathfrak{X})$, then we recover the original triple diagram \mathfrak{X} . The key property to keep in mind is that each face of \mathfrak{X} is homeomorphic to an open disk.

The strands of \mathfrak{X} run alongside the trips of G , implying that $\pi_{\mathfrak{X}} = \pi_G$. \square

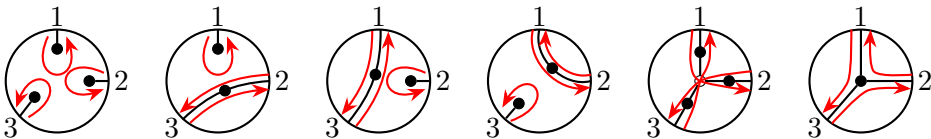


Figure 7.27. The six reduced normal plabic graphs with three boundary vertices, shown together with the corresponding triple diagrams, cf. Definition 7.5.9. The associated trip (resp., strand) permutations are precisely the six permutations of $\{1, 2, 3\}$.

In Theorem 7.7.3, we will characterize triple diagrams that correspond, under the bijection of Proposition 7.5.12, to *reduced* normal plabic graphs.

The bijective correspondence between triple diagrams and normal plabic graphs can be used to translate the move equivalence of triple diagrams (under the swivel moves, see Definition 7.5.5) into a version of the move equivalence of plabic graphs (cf. Definition 7.1.3) formulated entirely within the setting of normal plabic graphs:

Definition 7.5.13. The (*normal*) *urban renewal* move is the local transformation of normal plabic graphs described in Figure 7.28. (This differs slightly from Definition 2.5.2. In this chapter, we will consistently use the new definition.) Unlike the square move (M1), the normal urban renewal move does not require the vertices of the square to be trivalent. They can even be bivalent, see Figure 7.29.

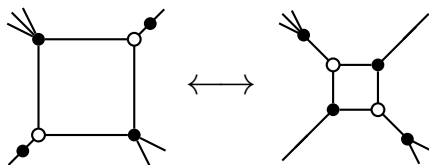


Figure 7.28. Normal urban renewal replaces one of these configurations by the other. In contrast to the square move of Figure 7.2, where each of the four vertices of the quadrilateral face must have exactly one incident edge leading outside the configuration, we allow each black vertex of the quadrilateral face to have 0 or more incident edges leading outside the configuration. Cf also Figure 7.29.

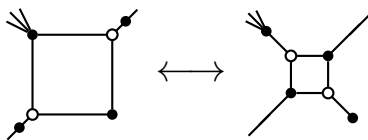


Figure 7.29. Special case of normal urban renewal: one of the black vertices is not incident to any edges leading outside the configuration.

Definition 7.5.14. The *normal flip move* is the local transformation shown in Figure 7.30. Ignoring the bivalent black vertices, this local move is the same as the (white) flip move for trivalent plabic graphs.

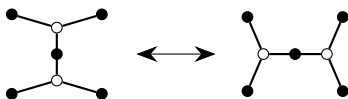


Figure 7.30. The normal flip move.

Lemma 7.5.15. *Let G and G' be normal plabic graphs related via a sequence of normal urban renewal moves and normal flip moves. Then $G \sim G'$.*

Proof. Each instance of normal urban renewal can be expressed as a square move (M1) together with (M2) and/or (M3) moves. Each normal flip move can be expressed as a combination of (M2) and (M3) moves. \square

Theorem 7.5.16. *Let G and G' be normal plabic graphs and let $\mathfrak{X} = \mathfrak{X}(G)$ and $\mathfrak{X}' = \mathfrak{X}(G')$ be the corresponding triple diagrams. Then the following are equivalent:*

- G and G' are related via a sequence of urban renewal moves and normal flip moves;
- \mathfrak{X} and \mathfrak{X}' are move-equivalent (i.e., related via swivel moves).

Proof. Figure 7.31 shows how one can translate back-and-forth between

- an arbitrary swivel move in a triple diagram and
- either an urban renewal move or the normal flip move in the corresponding normal plabic graph.

The latter choice depends on the orientations of the strands involved. \square

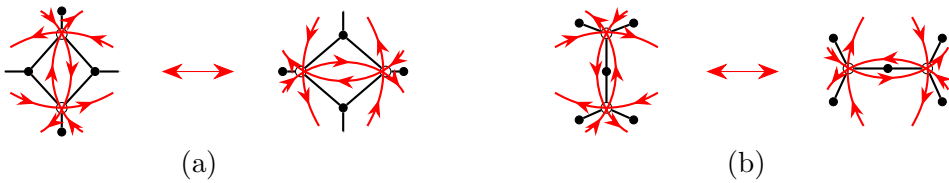


Figure 7.31. Depending on the orientations of the strands involved, a swivel move in a triple diagram may correspond to (a) an urban renewal move or (b) a normal flip move in the associated normal plabic graph.

We next generalize Definition 7.5.9 to arbitrary plabic graphs.

Definition 7.5.17. Let G be a plabic graph (not necessarily normal). The *generalized triple diagram* $\mathfrak{X}(G)$ associated to G is defined as follows. (To be precise, we define $\mathfrak{X}(G)$ up to move equivalence.) The recipe is essentially the same as in Definition 7.5.9, with the following additional rules dealing with non-trivalent white vertices:

- at a univalent white vertex in G , make a U-turn, see Figure 7.32;
- at a bivalent white vertex in G , go straight through, see Figure 7.32;
- at a white vertex v of degree ≥ 4 , replace v by a trivalent tree (with white vertices); then, at each of the vertices of the tree, apply the rule shown in Figure 7.25 on the right. See Figure 7.33.

Although the trivalent tree replacing v is not unique, all these trees are related to each other by flip moves, cf. Figure 7.12. Hence all triple diagrams constructed from them are move-equivalent to each other, cf. Figure 7.31(b) (remove the black vertex in the center).



Figure 7.32. Constructing a triple diagram around a white vertex of degree 1 or 2 in a general plabic graph.

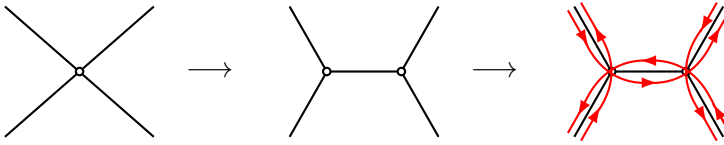


Figure 7.33. Constructing a triple diagram around a high-degree white vertex in a general plabic graph. We first replace this vertex by a trivalent tree, then construct the corresponding fragment of the triple diagram following the rule shown in Figure 7.25.

The following statement is immediate from the definitions.

Lemma 7.5.18. *Let G be a plabic graph. If the union of the strands in $\mathfrak{X}(G)$ and the boundary $\partial\mathbf{D}$ is connected, then $\mathfrak{X}(G)$ is a triple diagram in the sense of Definition 7.5.1.*

The connectedness condition in Lemma 7.5.18 does not hold in general. To be concrete, if G contains a cycle C all of whose vertices are black, then the strands located inside C are disconnected from the rest of $\mathfrak{X}(G)$.

Remark 7.5.19. Unfortunately, the extension of the definition of the triple diagram $\mathfrak{X}(G)$ described in Definition 7.5.17 does not allow a straightforward generalization of Theorem 7.5.16: move-equivalent plabic graphs do not necessarily yield move-equivalent triple diagrams. The only problematic local move is the one shown in Figure 7.34: contracting an edge connecting a white internal leaf to a white vertex of degree ≥ 3 removes a triple point in the associated triple diagram, thereby altering its move equivalence class.

This last complication prompts the following definition.

Definition 7.5.20. Let G and G' be plabic graphs. We write $G \overset{\circ}{\sim} G'$ if G and G' can be related to each other via a sequence of local moves (M1)–(M3) that does not include an instance of the (M3) move shown in Figure 7.34, cf. Remark 7.5.19.

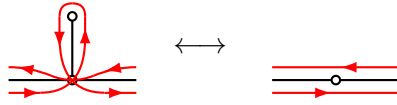


Figure 7.34. Contracting (or decontracting) an edge that connects a white internal leaf to a white vertex of degree ≥ 3 produces a move-equivalent triple diagram.

Lemma 7.5.21. *Let G and G' be plabic graphs such that $G \simeq G'$. Then the corresponding (generalized) triple diagrams $\mathfrak{X}(G)$ and $\mathfrak{X}(G')$ are move equivalent (i.e., related to each other via swivel moves).*

We note that $\mathfrak{X}(G)$ and $\mathfrak{X}(G')$ are defined up to move equivalence, so the statement that they are move-equivalent to each other makes sense.

Proof. It is straightforward to verify, case by case, that each of the local moves (M1)–(M3), with the exception of the move shown in Figure 7.34, either leaves the associated (generalized) triple diagram invariant or applies a swivel move to it (more precisely, to any of the possible diagrams obtained using the construction in Definition 7.5.17). To be specific:

- a square move (M1) translates into a swivel move, see Figure 7.31(a);
- both the move (M2) and a black (de)contraction move (M3) leave the triple diagram invariant (up to isotopy);
- a white (de)contraction move (M3), other than the instance shown in Figure 7.34, translates into a swivel move, see Figure 7.31(b) (remove the black vertex in the center). \square

Corollary 7.5.22. *Let G and G' be normal plabic graphs. The following are equivalent:*

- (1) $G \simeq G'$;
- (2) G and G' are related via a sequence of normal urban renewal moves and normal flip moves;
- (3) $\mathfrak{X}(G)$ and $\mathfrak{X}(G')$ are move-equivalent (in the sense of Definition 7.5.5).

Proof. The implication (2) \Rightarrow (1) is an easy enhancement of Lemma 7.5.15. The equivalence (2) \Leftrightarrow (3) was established in Theorem 7.5.16. The implication (1) \Rightarrow (3) was proved in Lemma 7.5.21. \square

We note the similarity between Corollary 7.5.22 and Theorem 7.3.5.

7.6. Minimal triple diagrams

Definition 7.6.1. A triple diagram is called *minimal* if it has no more triple points than any other triple diagram with the same strand permutation.

We will show in Section 7.7 that minimal triple diagrams are the natural counterparts of reduced normal plabic graphs.

Much of this section is devoted to the proof of the following key result.

Theorem 7.6.2. *Any two minimal triple diagrams with the same strand permutation are move-equivalent to each other.*

Lemma 7.6.3. *If a triple diagram \mathfrak{X} is minimal, then so is every triple diagram move-equivalent to \mathfrak{X} .*

Proof. It is easy to see that a swivel move preserves both the number of triple points and the strand permutation. The claim follows. \square

We next describe certain “bad features” (of a triple diagram) and show that they cannot occur in a minimal triple diagram.

Definition 7.6.4. A strand in a triple diagram that intersects itself forms a *monogon*. A pair of strands that intersect at two points x and y form either a *parallel digon* or *anti-parallel digon*, depending on whether their segments connecting x and y run in the same or opposite direction, see Figure 7.35. We use the term *badgon* to refer to either a monogon or a parallel digon.

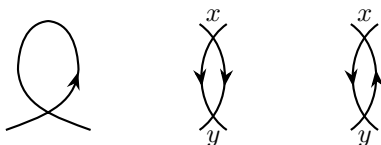


Figure 7.35. A monogon, a parallel digon, and an anti-parallel digon. The actual picture will contain (potentially many) additional strands and intersections.

Lemma 7.6.5. *A triple diagram without badgons has no closed strands.*

Proof. Let \mathfrak{X} be a triple diagram without badgons. Since \mathfrak{X} does not contain monogons, no strand of \mathfrak{X} can intersect itself. Suppose that \mathfrak{X} contains a closed strand S . Let T be another strand of \mathfrak{X} intersecting S at points x and y ; such T exists since \mathfrak{X} must be connected to the boundary $\partial\mathbf{D}$. Then the segment of T between x and y together with one of the segments of S connecting x and y form a parallel digon, which is a contradiction. \square

Lemma 7.6.6. *A minimal triple diagram does not contain badgons. Therefore (cf. Lemma 7.6.5) it does not contain closed strands.*

Proof. Let \mathfrak{X} be a triple diagram containing a monogon, i.e., a strand S with a self-intersection at a triple point v . Construct the triple diagram \mathfrak{X}' by deforming \mathfrak{X} around v so that S “spins off” a closed strand while the triple point disappears, see Figure 7.36. (If the spun-off portion is disconnected from the rest of \mathfrak{X} , then remove it altogether.) The triple diagram \mathfrak{X}' has the same strand permutation as \mathfrak{X} but fewer triple points; thus \mathfrak{X} is not minimal.

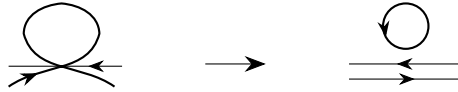


Figure 7.36. In the presence of a monogon, we can reduce the number of triple points while keeping the same strand permutation. The triple diagram may contain additional strands intersecting the monogon, as well as additional points of self-intersection.

Now suppose that \mathfrak{X} does not contain monogons but does contain two strands S and T that form a parallel digon. Say, S and T contain segments \overline{S} and \overline{T} that run from a triple point x to a triple point y . Let U (resp., V) be the third strand passing through x (resp., y). We then deform \mathfrak{X} around both x and y by smoothing each of the two triple points: the strands U and V continue to go straight through, whereas the endpoints of \overline{S} (resp., \overline{T}) get connected to T (resp., S). Thus, the strands S and T swap their segments \overline{S} and \overline{T} with each other (with appropriate smoothings), the overall connectivity (i.e., the strand permutation) is preserved, and the triple points at x and y disappear. (If the diagram becomes disconnected from $\partial\mathbf{D}$, then remove the disconnected portion.) We then conclude that \mathfrak{X} was not minimal. \square

Definition 7.6.7. Let S be an arc in a triple diagram, i.e., a strand whose endpoints s and t lie on the boundary of the ambient disk \mathbf{D} . We call S *boundary-parallel* if it runs along a segment I of the boundary $\partial\mathbf{D}$ between s and t (in either direction), so that every other strand with an endpoint inside I runs directly to or from S , without any triple crossings in between. See Figure 7.37.

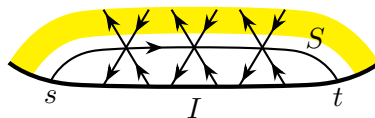


Figure 7.37. A boundary-parallel strand S in a triple diagram.

We next describe a particular way to construct, for any given permutation π , a triple diagram whose strand permutation is π .

Definition 7.6.8. Let π be a permutation of b letters $1, \dots, b$. A triple diagram in the disk \mathbf{D} is called *standard* (for π) if it can be constructed using the following recursive process. (The process involves some choices, so a standard diagram for π is not unique.)

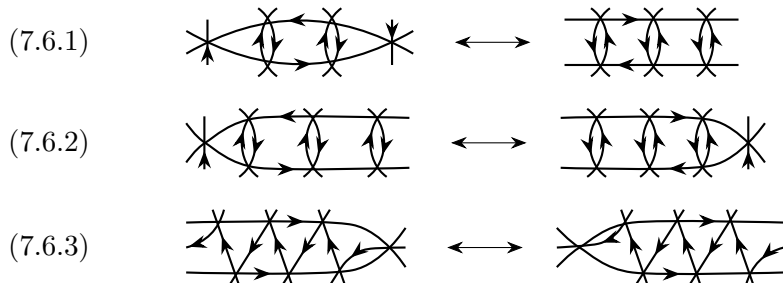
We place b boundary vertices on the boundary $\partial\mathbf{D}$ and label them $1, \dots, b$ clockwise. Next to each boundary vertex v , we mark two endpoints of the future strands: a source endpoint that precedes v in the clockwise order and a target endpoint that follows v in this order. We know which source is to be matched to which target by the strand permutation π . Each such pair of endpoints divides the circle $\partial\mathbf{D}$ into two intervals. Let us partially order these $2b$ intervals by inclusion and select a *minimal interval* I with respect to this partial order.

We start constructing the triple diagram by running a boundary-parallel strand S along the interval I , introducing a triple crossing for each pair of strands that need to terminate in the interior of I , as shown in Figure 7.37. There will always be an even number (possibly zero) of strands to cross over, so the construction will proceed without a hitch.

Let \mathbf{D}' be the disk obtained from \mathbf{D} by removing the region between the boundary segment I and the strand S together with a small neighborhood of S ; so \mathbf{D}' is the shaded region in Figure 7.37. We accordingly remove S and its endpoints from the original pairing of the in- and out-endpoints, and swap each pair that S crossed over. This yields $2(b-1)$ endpoints on the boundary of \mathbf{D}' ; note that the in- and out-endpoints alternate, as before. We then determine the new pairing of these endpoints (thus, a new strand permutation, after an appropriate renumbering) and recursively continue the process in \mathbf{D}' until the desired (standard) triple diagram is constructed.

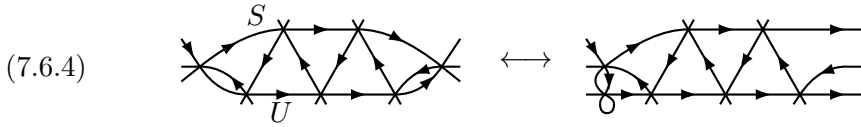
We shall keep in mind that a standard triple diagram is constructed by choosing a sequence of minimal intervals.

Exercise 7.6.9. For each of the three pairs of triple diagrams shown below, demonstrate that the two diagrams are move-equivalent to each other, i.e., related via a sequence of swivel moves.



(In each of the three cases, the central section can involve an arbitrary number of repetitions.)

Exercise 7.6.10. Use (7.6.3) to prove the move equivalence (7.6.4) below:



Lemma 7.6.11. Let \mathfrak{X} be a triple diagram such that no triple diagram move-equivalent to \mathfrak{X} contains a monogon. Then the following statements hold:

- (i) No triple diagram move-equivalent to \mathfrak{X} has a badgon or a closed strand.
- (ii) Let I be a minimal interval for the strand permutation associated with \mathfrak{X} . Then \mathfrak{X} is move-equivalent to a diagram \mathfrak{X}' in which the strand connecting the endpoints of I is boundary-parallel along I .

Proof. We will simultaneously prove statements (i) and (ii) by induction on the number of triple points in \mathfrak{X} . Thus, we assume that both (i) and (ii) hold for triple diagrams that have fewer triple points than \mathfrak{X} .

We first prove (i). Suppose that a triple diagram $\mathfrak{X}' \sim \mathfrak{X}$ contains (non-self-intersecting) strands S and U forming a parallel digon. The strand S cuts the disk \mathbf{D} into two regions. Let R be the region containing the digon, with a small neighbourhood of S removed. Since the boundaries of the faces of \mathfrak{X}' are consistently oriented, the same is true for the portion of \mathfrak{X}' contained inside R , so this portion can be viewed as a (smaller) triple diagram. Suppose that U bounds a minimal interval within S (viewed as a portion of the boundary of R). Then by the induction assumption, U can be moved to be boundary-parallel to S . Since S and U are co-oriented, we get the picture on the left-hand side of (7.6.4) (with U running horizontally at the bottom). Applying (7.6.4), we obtain a monogon, a contradiction.

If the subinterval of S cut out by U is not minimal, then there is a strand T that cuts across S twice, creating a minimal interval within S and forming a digon inside R . We may assume that this digon is anti-parallel (or else replace U by T and repeat). By the induction assumption, we can apply swivel moves inside R to make T boundary-parallel to S . We then apply (7.6.1) to remove the digon, as shown in Figure 7.38. Repeating this operation if necessary, we obtain a triple diagram in which U bounds a minimal interval within S ; we then argue as above to arrive at a contradiction.

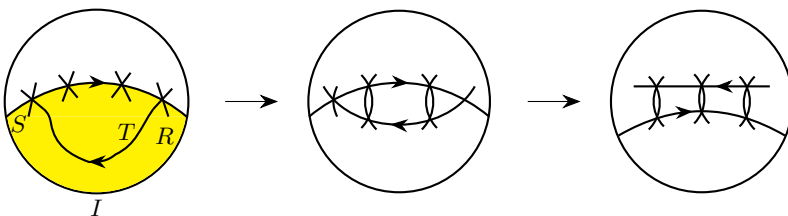


Figure 7.38. Removing double intersections with S .

Thus, no triple diagram $\mathfrak{X}' \sim \mathfrak{X}$ contains badgons. By Lemma 7.6.5, we conclude that any such \mathfrak{X}' does not contain closed strands either. This completes the induction step for statement (i).

We now proceed to proving statement (ii). In addition to the induction assumption for (ii), we may assume that neither \mathfrak{X} nor any triple diagram move-equivalent to \mathfrak{X} contains a badgon or a closed strand.

Let S be the strand connecting the endpoints of the minimal interval I .

Step 1: Removing double intersections with S , see Figure 7.38. Let R be the region between the strand S and the interval I , with a small neighborhood of S removed. Suppose there is a strand that intersects S more than once. Among such strands, take one that cuts out a minimal interval along the boundary of R . Let T denote the segment of this strand contained in R . The portion of \mathfrak{X} contained inside R has fewer triple crossings than \mathfrak{X} , so by the induction assumption, we can make T boundary-parallel to S by applying swivel moves inside R . Now T and S form a (necessarily anti-parallel) digon, which we then remove using (7.6.1). We repeat this procedure until there are no strands left that intersect S more than once. Since the number of triple points along S decreases each time, the process terminates.

Step 2: Combing out the triple crossings. At this stage, no strand crosses S more than once. Since I is minimal, no strand has both ends at I . Since \mathfrak{X} contains no closed strands, every (non-self-intersecting) strand appearing between S and I must start or end at a point in I and cross S . Suppose that S is not boundary-parallel. Then there exists a strand T with an endpoint at I that passes through a triple point before hitting S . Among all such T , choose the one with the leftmost endpoint along I , cf. Figures 7.39 and 7.40 on the left. Let R be the part of the region between I and S that lies to the right of any strand T' located to the left of T . (By our choice of T , all such strands T' run directly from I to S , with no crossings in between.) As we have eliminated all double intersections with S , the interval corresponding to T (looking to the left) is minimal inside R . We can therefore use the induction assumption inside R to make T boundary-parallel.

What we do next depends on the orientation of T relative to S . If T is anti-parallel to S , as in Figure 7.39, then we apply (7.6.2) to make T run directly to S . If T is parallel to S , as in Figure 7.40, then we apply (7.6.3).

We repeat this step until S is boundary-parallel. □

Lemma 7.6.12. *For a triple diagram \mathfrak{X} , the following are equivalent:*

- (a) *Any diagram \mathfrak{X}' move-equivalent to \mathfrak{X} does not contain a monogon.*
- (b) *\mathfrak{X} is move-equivalent to any standard triple diagram with the same strand permutation.*
- (c) *\mathfrak{X} is minimal.*

In particular, any standard triple diagram is minimal.

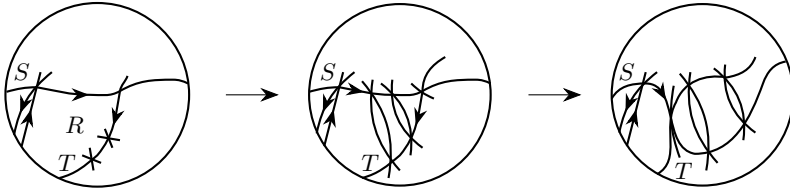


Figure 7.39. Combing out the triple crossings: the anti-parallel case.

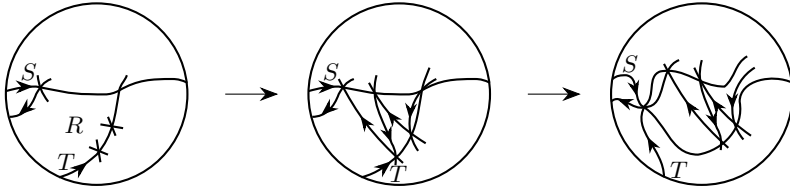


Figure 7.40. Combing out the triple crossings: the parallel case.

Proof. The implication (c) \Rightarrow (a) follows from Lemmas 7.6.3 and 7.6.6. To prove the implication (a) \Rightarrow (b), choose a sequence of minimal intervals and repeatedly apply Lemma 7.6.11. We have now established (c) \Rightarrow (b), so any minimal triple diagram is move-equivalent to any standard triple diagram with the same strand permutation. It follows by Lemma 7.6.3 that any standard triple diagram is minimal, hence so is any diagram move-equivalent to a standard one. Thus (b) \Rightarrow (c) is proved. \square

Proof of Theorem 7.6.2. By Lemma 7.6.12, any two minimal triple diagrams with strand permutation π are move-equivalent to any standard diagram with strand permutation π , and therefore to each other. \square

Lemma 7.6.13. *Let \mathfrak{X} and \mathfrak{X}' be triple diagrams related by a swivel move. If \mathfrak{X} contains a badgon, then so does \mathfrak{X}' .*

Proof. We label the strands and the triple points involved in this swivel move by a, b, c, d , and x, y , as shown in Figure 7.41.

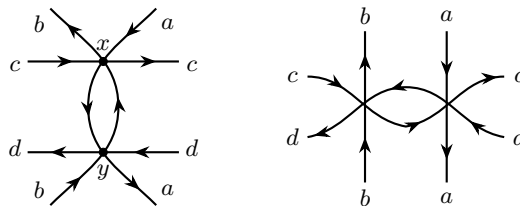


Figure 7.41. A swivel move relating \mathfrak{X} and \mathfrak{X}' .

If \mathfrak{X} contains a badgon that involves neither x nor y , then this badgon persists in \mathfrak{X}' .

Suppose \mathfrak{X} contains a monogon whose self-intersection point is (say) x . Thus, two of the strands $\{a, b, c\}$ coincide. If $a = c$ (resp., $b = c$), then the same monogon persists in \mathfrak{X}' because in Figure 7.41, strands a and c (resp., b and c) intersect in both \mathfrak{X} and \mathfrak{X}' .

If, on the other hand, $a = b$, then \mathfrak{X}' has a parallel digon, see Figure 7.42.

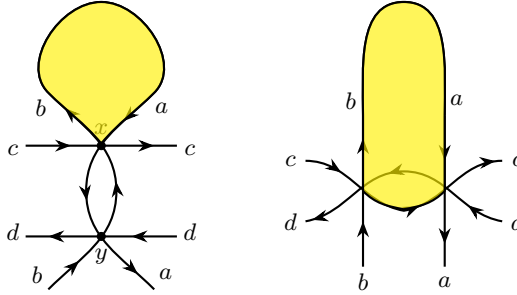


Figure 7.42. A monogon in \mathfrak{X} results in a parallel digon in \mathfrak{X}' .

From now on, we can assume that there is no monogon in \mathfrak{X} . Suppose \mathfrak{X} has a parallel digon whose two intersection points include x but not y . The sides of this parallel digon are either $\{a, b\}$ or $\{a, c\}$ or $\{b, c\}$. The last two cases are easy because such a parallel digon will persist in \mathfrak{X}' , since the strands a and c (resp., b and c) intersect in both \mathfrak{X} and \mathfrak{X}' .

Now suppose that our parallel digon has sides a and b , see Figure 7.43 on the left. (If the strands a and b go to the left and meet again there, then we get the same picture but with the roles of x and y interchanged.) Note that the end of strand a shown inside the digon must extend outside of it, but it cannot intersect a , as this would create a monogon. So strand a must intersect strand b again, see Figure 7.43 in the middle. Then, after the swivel move, we get a parallel digon as shown in Figure 7.43 on the right.

Finally, suppose there is a parallel digon in \mathfrak{X} whose two intersection points are x and y . We can assume it is oriented from x to y . The two arcs of the parallel digon should come from the following list:

- (aa) the arc along a from x to y ;
- (bb) the arc along b from x to y ;
- (cd) an arc leaving x along c , and returning to y along d (so $c = d$);
- (cb) an arc leaving x along c , and returning to y along b (so $c = b$);
- (bd) an arc leaving x along b , and returning to y along d (so $b = d$).

In case (bb), we get a closed strand; it will persist in \mathfrak{X}' and yield a badgon by Lemma 7.6.5. In cases (cb) and (bd), we get a monogon, contradicting our assumption. The remaining case is when the parallel digon has sides (aa) and (cd), in which case we get a monogon in \mathfrak{X}' . (The picture is like Figure 7.42, with the roles of \mathfrak{X} and \mathfrak{X}' swapped and some strands relabeled.)

□

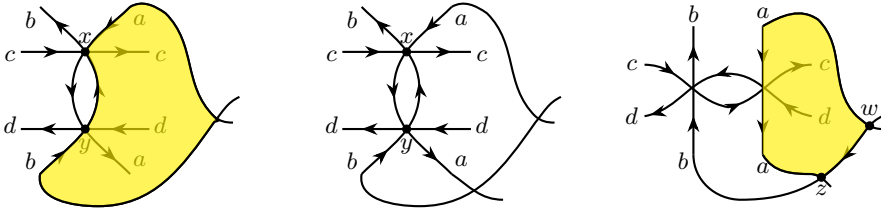


Figure 7.43. Persistence of parallel digons under swivel moves.

Theorem 7.6.14. *A triple diagram is minimal if and only if it has no badgons.*

Proof. The “only if” direction is Lemma 7.6.6. The “if” direction follows from Lemma 7.6.13 and Lemma 7.6.12 (implication (a) \Rightarrow (c)). \square

Lemma 7.6.15. *Assume that a triple diagram \mathfrak{X} is not minimal. Then there exists a diagram \mathfrak{X}' move-equivalent to \mathfrak{X} that contains a hollow monogon.*

Proof. We will argue by induction on the number of faces in \mathfrak{X} . If this number is 1 or 2, then the claim is vacuously true.

By Lemma 7.6.12, there exists $\mathfrak{X}' \sim \mathfrak{X}$ such that \mathfrak{X}' has a monogon. Let M be the segment of a strand in \mathfrak{X}' that forms a monogon; we may assume M does not intersect itself except at its endpoints (or else replace M by its subsegment). If the monogon encircled by M is hollow, we are done. Otherwise, consider the disk \mathbf{D}_\circ obtained by removing a small neighborhood of M from the interior of the monogon. Let \mathfrak{X}'_\circ denote the portion of \mathfrak{X}' contained in \mathbf{D}_\circ ; this is a triple diagram with fewer faces than \mathfrak{X}' (or equivalently \mathfrak{X}).

The rest of the argument proceeds by showing that either we can apply local moves to \mathfrak{X}'_\circ to create a hollow monogon inside \mathbf{D}_\circ or we can apply moves to reduce the number of faces inside the monogon encircled by M (eventually producing a hollow monogon). If \mathfrak{X}'_\circ is not minimal, then the induction assumption applies, so we can transform \mathfrak{X}'_\circ (thus \mathfrak{X}' or \mathfrak{X}) into a move-equivalent triple diagram containing a hollow monogon. Therefore, we may assume that \mathfrak{X}'_\circ is minimal. Let M_\circ denote the interval obtained from the boundary of \mathbf{D}_\circ by removing a point located near the vertex of our monogon. Let $I \subset M_\circ$ be a minimal interval of the triple diagram \mathfrak{X}'_\circ . Since this triple diagram is minimal, we can, by virtue of Lemma 7.6.12 (or Lemma 7.6.11), apply local moves inside \mathbf{D}_\circ to transform \mathfrak{X}'_\circ into a triple diagram in which the strand T connecting the endpoints of I is boundary-parallel to I . Let us now look at the digon formed by T and the portion of M that runs along I . If this digon is anti-parallel, then we can push T outside the monogon as in Figure 7.38, reducing the number of faces enclosed by M . If, on the other hand, the digon is parallel, then we can use (7.6.4) to create a hollow monogon. \square

7.7. From minimal triple diagrams to reduced plabic graphs

In this section, we use the machinery of triple diagrams and normal plabic graphs to prove Proposition 7.4.22 and Theorem 7.4.25.

Lemma 7.7.1. *A normal plabic graph contains no collapsible trees.*

Proof. All internal leaves in a normal plabic graph G are black. Whatever (M2)–(M3) moves we apply to a tree, it will always have a black leaf (so it can't collapse to a white root or lollipop), and it will always have a white vertex of degree at least 3 (so it can't collapse to a black root or lollipop). \square

Lemma 7.7.2. *Let G be a non-reduced normal plabic graph. Then there exists a plabic graph $G' \simeq G$ (cf. Definition 7.5.20) containing one of the forbidden configurations shown in Figure 7.18.*

Proof. Suppose G has an internal (necessarily black) leaf u that is not a lollipop. Let v be the unique (white, trivalent) vertex adjacent to u . This gives us a forbidden configuration as in Figure 7.18(d). (Note that by Lemma 7.7.1, G has no collapsible trees.)

If, on the other hand, G has no such internal leaves, then by Proposition 7.4.9, G can be transformed, via local moves that do not create leaves, into a graph containing a hollow digon. \square

Recall that by Proposition 7.5.12, the map $G \rightarrow \mathfrak{X}(G)$ defined in Definition 7.5.9 gives a bijection between normal plabic graphs and triple diagrams with the same number of boundary vertices; moreover, this bijection preserves the associated (resp., trip or strand) permutation.

Theorem 7.7.3. *A normal plabic graph G is reduced if and only if the triple diagram $\mathfrak{X}(G)$ is minimal. Thus the map $G \mapsto \mathfrak{X}(G)$ restricts to a bijection between reduced normal plabic graphs and minimal triple diagrams.*

Proof. Suppose $\mathfrak{X}(G)$ is not minimal. By Lemma 7.6.15, there is a triple diagram $\mathfrak{X}' \sim \mathfrak{X}(G)$ such that \mathfrak{X}' has a hollow monogon. By Proposition 7.5.12, we have $\mathfrak{X}' = \mathfrak{X}(G')$ for some normal plabic graph G' . Moreover, by Corollary 7.5.22, G and G' are move equivalent. The hollow monogon in \mathfrak{X}' corresponds in the normal graph G' to one of the configurations shown in Figure 7.44: either a hollow digon or a black leaf adjacent to a white trivalent vertex. Either way, G' contains one of the forbidden configurations from Figure 7.18 (cf. Lemma 7.7.1), so G is not reduced.

Going in the other direction, suppose that a normal plabic graph G is not reduced. By Lemma 7.7.2, there exists $G' \simeq G$ containing a forbidden configuration. By Lemma 7.5.21, the triple diagram $\mathfrak{X}(G)$ is move-equivalent

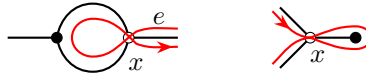


Figure 7.44. A hollow monogon in a triple diagram yields a forbidden configuration in the corresponding normal plabic graph, cf. Figure 7.18.

to the (generalized) triple diagram $\mathfrak{X}(G')$. Since $\mathfrak{X}(G)$ is connected, so is $\mathfrak{X}(G')$. It follows by Lemma 7.5.18 that $\mathfrak{X}(G')$ is an honest triple diagram.

The remaining argument depends on the type of a forbidden configuration present in G' . Since G is normal and $G' \simeq G$, it follows that G' has no white leaves. If G' contains a digon whose vertices are of the same color, then $\mathfrak{X}(G')$ has a closed strand; hence $\mathfrak{X}(G')$ is not minimal (by Lemma 7.6.6) and neither is $\mathfrak{X}(G)$. Finally, if G' contains one of the configurations shown in Figure 7.44, then $\mathfrak{X}(G')$ contains a monogon, hence is not minimal. \square

Lemma 7.7.4. *Let G be a reduced plabic graph that does not contain a white lollipop, nor a tree that collapses to a white lollipop. Then G is move-equivalent to a normal plabic graph.*

See Figure 7.45.

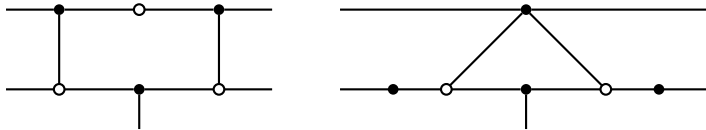


Figure 7.45. A reduced plabic graph G and a normal plabic graph move-equivalent to G .

Proof. We use induction on the number of faces of G . Note that each local move keeps this number invariant. We begin by collapsing all collapsible trees (cf. Definition 7.4.1) and removing all bivalent vertices. The resulting plabic graph has no white leaves, since a white leaf would either be a lollipop or else be adjacent to a black vertex of degree ≥ 3 , which is impossible since the plabic graph at hand is reduced and has no collapsible trees.

We then split each white vertex of degree ≥ 4 into a tree made of trivalent white vertices. After that, we insert a bivalent black vertex in the middle of each edge with both endpoints white, as well as near each boundary vertex connected to a white vertex. By an abuse of notation, we keep calling our plabic graph G , even as it undergoes these and subsequent transformations.

It remains to contract the edges with both endpoints black to make the graph bipartite. This step may however be problematic if such an edge e is a loop connecting some black vertex v to itself. We will demonstrate that this in fact cannot happen.

If e encloses a face (i.e., there are no other vertices/edges of G inside e), then we can insert a black vertex into e and obtain a double edge, contradicting the fact that G is reduced. Now suppose that e encloses some nontrivial subgraph of G . Let \mathbf{D}' be the region bounded by e . We split v into two vertices v_1 and v_2 using an (M3) move, so that v_1 stays incident to e and to the edges located outside \mathbf{D}' whereas v_2 is incident to the edges inside \mathbf{D}' . See Figure 7.46.

We thus obtain a subgraph G' , viewed as a plabic graph in \mathbf{D}' with a single boundary vertex v_1 . The plabic graph G' must be reduced, or else G would not be. Moreover G' has fewer faces than G . Also, G' does not collapse to a white lollipop (even if v_2 is bivalent), because this would result (after the collapse) in a forbidden configuration in G . (We note that G has no collapsible trees.) Thus, the induction hypothesis applies, so we can transform G' via local moves into a normal graph G'' . Since G'' is reduced, its triple diagram $\mathfrak{X}(G'')$ must be minimal by Theorem 7.7.3. Given that $\mathfrak{X}(G'')$ only has one in- and one out-endpoint, this means that $\mathfrak{X}(G'')$ consists of a single strand connecting these endpoints to each other, with no triple points. In other words, the normal graph G'' is a black lollipop at v_1 . We then contract it into v_1 , creating a loop enclosing a face, and arrive at a contradiction with G being reduced. \square

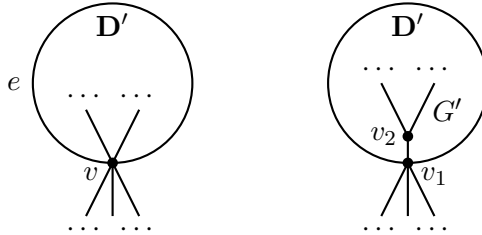


Figure 7.46. Excluding a loop e based at a black vertex v .

Proof of Proposition 7.4.22. Let G be a reduced plabic graph such that $\pi_G(i) = i$. We need to show that the connected component of G containing the boundary vertex i collapses to a lollipop at i , cf. Definition 7.4.1.

Suppose otherwise. Without loss of generality, we can assume that G has no trees collapsing to other lippops either. Since G is reduced, Lemma 7.7.4 applies, so G is move-equivalent to a normal plabic graph G' . The trip permutations of G and G' coincide with each other (by Exercise 7.4.19) and with the strand permutation of the triple diagram $\mathfrak{X}(G')$ (by Proposition 7.5.12). Since G is reduced, so is G' ; hence $\mathfrak{X}(G')$ is minimal by Theorem 7.7.3.

Let d be the degree of the black vertex adjacent to the boundary vertex i in G' . If $d = 1$, then there is a sequence of local moves relating the component of G containing i to the black lollipop at i in G' . Since local moves preserve the number of internal faces, and a black lollipop has no

internal faces, no (M1) move appears in the sequence of moves. Therefore this component must be a (collapsible) tree and we are done. If $d = 2$ (see Figure 7.47 on the left), then $\pi_G(i) = i$ implies that $\mathfrak{X}(G')$ has a monogon, so it cannot be minimal, cf. Lemma 7.6.6. If $d \geq 3$, then we get a parallel digon (see Figure 7.47 on the right), again contradicting the minimality of $\mathfrak{X}(G')$.

□



Figure 7.47. The vicinity of i in G' .

Proof of Theorem 7.4.25. Let G and G' be reduced plabic graphs. If $G \sim G'$, then $\tilde{\pi}_G = \tilde{\pi}_{G'}$ by Exercise 7.4.24. We need to show the converse.

Let G and G' be reduced plabic graphs such that $\tilde{\pi}_G = \tilde{\pi}_{G'}$. If this decorated permutation has a fixed point at some vertex i , then by Proposition 7.4.22, after applying local moves if needed, both G and G' have a lollipop (of the same color) in position i . We can delete this lollipop in both graphs; the resulting graphs are still reduced, and their decorated trip permutations still coincide. So without loss of generality, we may assume that $\tilde{\pi}_G = \tilde{\pi}_{G'}$ has no fixed points and correspondingly G and G' have no trees collapsing to lollipops. Applying local moves as needed, we can furthermore assume, in light of Lemma 7.7.4, that both G and G' are normal. Since they are also reduced, Theorem 7.7.3 implies that the triple diagrams $\mathfrak{X}(G)$ and $\mathfrak{X}(G')$ are minimal. By Proposition 7.5.12, we moreover have $\pi_{\mathfrak{X}(G)} = \pi_G = \pi_{G'} = \pi_{\mathfrak{X}(G')}$. Invoking Theorem 7.6.2, we conclude that $\mathfrak{X}(G)$ and $\mathfrak{X}(G')$ are move-equivalent. Then by Corollary 7.5.22, G and G' are move-equivalent as well. □

Remark 7.7.5. As we have seen, A. Postnikov's theory of plabic graphs [21] is closely related to D. Thurston's theory of triple diagrams [24]. In particular, reduced plabic graphs are essentially minimal triple diagrams in disguise. While we have not discussed it here, there are some *reduction moves* that can be repeatedly applied to a non-reduced plabic graph (resp., a non-minimal triple diagram) in order to—eventually—make it reduced (resp., minimal). Here the two theories diverge: reduction moves for triple diagrams preserve the strand permutation, but reduction moves for plabic graphs do not preserve the trip permutation. In spite of that, reduction moves for plabic graphs fit into the theory of the totally nonnegative Grassmannian, as they are compatible with its cell decomposition, cf. [21, Section 12]. We will discuss this in the next chapter.

7.8. The bad features criterion

Here we provide an algorithm for deciding whether a plabic graph is reduced or not. We first explain (see Definition 7.8.2) how to transform an arbitrary plabic graph G into a normal plabic graph $N(G)$ move-equivalent to G (or conclude that G is not reduced). We then use a criterion based on Theorem 7.7.3 to determine whether $N(G)$ (hence G) is reduced or not.

Lemma 7.8.1. *Let G be a reduced plabic graph. Then G has no roundtrips. Also, G has no loops, i.e., edges whose endpoints coincide.*

Proof. We can assume that G does not contain white lollipops or trees that collapse to white lollipops. (Collapsing such trees and removing lollipops does not affect whether a graph is reduced or whether it has a roundtrip.) Now by Lemma 7.7.4, G is move-equivalent (up to the removal of some white lollipops) to a normal plabic graph G' . Since G' is reduced, $\mathfrak{X}(G')$ is minimal (see Theorem 7.7.3). Hence $\mathfrak{X}(G')$ has no closed strands (see Lemma 7.6.6), so G' has no roundtrips. Since roundtrips persist under local moves, G has no roundtrips either.

Suppose G has a loop e based at a black (resp., white) vertex. (Some edges and vertices might be enclosed by e .) Then the trip that traverses e clockwise (resp., counterclockwise) is a roundtrip, a contradiction. \square

Definition 7.8.2. Let G be a plabic graph. The following algorithm is similar to the procedure employed in the proof of Lemma 7.7.4. It either determines that G is not reduced, or outputs a normal plabic graph $N(G)$ which, up to the addition/removal of lollipops, is move-equivalent to G . In the latter scenario, the plabic graph $N(G)$ —hence the original graph G —may be either reduced or not.

At each stage of the algorithm, the plabic graph G undergoes some transformations that do not affect whether it is reduced.

Stage 1. Use moves (M2)–(M3) to collapse all collapsible trees in G .

Stage 2. Use moves (M2) to remove all bivalent vertices.

Stage 3. Remove all lollipops.

Stage 4. If G has an internal leaf u , then let v be the vertex adjacent to u . By construction, $\deg(v) \geq 3$. Since G has no collapsible trees, we conclude that u and v are of different color and G is not reduced.

If G has no internal leaves, then each internal vertex has degree ≥ 3 .

Stage 5. Use moves (M3) to contract all edges with both endpoints black. If at any point G has a loop, then it is not reduced, by Lemma 7.8.1.

Stage 6. Use moves (M3) to replace each white vertex by a trivalent tree with white vertices.

Stage 7. Use moves (M2) to insert a black vertex into every edge with no black endpoints. The resulting plabic graph $N(G)$ is normal.

Definition 7.8.3. If a trip passes through an edge e of a plabic graph twice (in the opposite directions), we call this an *essential self-intersection*.

If the edges e_1 and e_2 are such that there are two distinct trips each of which passes first through e_1 and then through e_2 , we call this a *bad double crossing*.

We use the term *bad features* to collectively refer to

- roundtrips (see Definition 7.4.12),
- essential self-intersections, and
- bad double crossings.

These notions are illustrated in Figure 7.48.

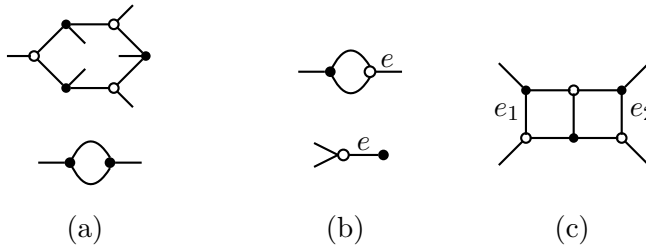


Figure 7.48. Plabic graph fragments representing “bad features:” (a) a roundtrip; (b) essential self-intersection; (c) bad double crossing.

Lemma 7.8.4. *A normal plabic graph G has a bad feature if and only if the associated triple diagram $\mathfrak{X}(G)$ has a badgon.*

Proof. Let G be a normal plabic graph. The strands in the triple diagram $\mathfrak{X} = \mathfrak{X}(G)$ closely follow the trips in G . Therefore \mathfrak{X} has a closed strand if and only if G has a roundtrip.

If G has an essential self-intersection (resp., a bad double crossing), then \mathfrak{X} has a monogon (resp., a parallel digon). To see that, take each edge e involved in a bad feature and consider the white end v of e . The strands corresponding to the trips involved in the bad feature will intersect at v ; thus v will be a vertex of the corresponding badgon. Cf. Figures 7.44 and 7.49.

Conversely, suppose that \mathfrak{X} has a monogon with self-intersection corresponding to the white vertex v of G . There are three strand segments of \mathfrak{X} that pass through v , each running along two distinct edges incident to v ; because we have a self-intersection, two of these strands segments are part of the same strand s . Since v is trivalent, the pigeonhole principle implies

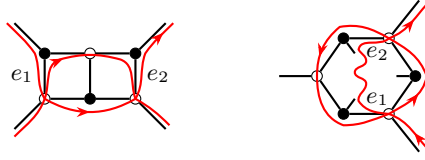


Figure 7.49. A bad double crossing in G yields a parallel digon in $\mathfrak{X}(G)$.

that two of the four edges that s runs along must coincide. This yields an essential self-intersection in G . A similar argument shows that if \mathfrak{X} has a parallel digon, then G has a bad double crossing. \square

Corollary 7.8.5. *Let G be a normal plabic graph. Let $\mathfrak{X} = \mathfrak{X}(G)$ be the corresponding triple diagram. Then the following are equivalent:*

- G is reduced;
- \mathfrak{X} is minimal;
- G has no bad features;
- \mathfrak{X} has no badgons.

Proof. By Theorem 7.7.3, G is reduced if and only if \mathfrak{X} is minimal. By Theorem 7.6.14, \mathfrak{X} is minimal if and only if \mathfrak{X} has no badgons. By Lemma 7.8.4, \mathfrak{X} has no badgons if and only if G has no bad features. \square

Corollary 7.8.5 provides the following criterion, which is a version of [21, Theorem 13.2].

Theorem 7.8.6. *A normal plabic graph is reduced if and only if it does not contain any bad features.*

For example, any plabic graph containing one of the fragments shown in Figure 7.48 is necessarily not reduced.

Remark 7.8.7. For *any* plabic graph G , Theorem 7.8.6 can be used in conjunction with the procedure described in Definition 7.8.2 to determine whether G is reduced or not.

Remark 7.8.8. Recall from Remark 2.3.4 that a factorization (not necessarily reduced) of an element of a symmetric group into a product of simple reflections can be represented by (a version of) a wiring diagram. As plabic graphs can be viewed as generalizations of wiring diagrams (see Example 7.2.4), reduced plabic graphs may be viewed as a generalization of reduced expressions. In this context, the criterion of Theorem 7.8.6 corresponds to the condition that each pair of lines in the wiring diagram intersect at most once.

7.9. Affine permutations

By Theorem 7.4.25, move equivalence classes of reduced plabic graphs are labeled by decorated permutations. An alternative (sometimes more useful) labeling utilizes $((a, b)$ -bounded) *affine permutations*, introduced and studied in this section.

Definition 7.9.1. For a decorated permutation $\tilde{\pi}$ on b letters, we say that $i \in \{1, \dots, b\}$ is an *anti-excedance* of $\tilde{\pi}$ if either $\tilde{\pi}^{-1}(i) > i$ or if $\tilde{\pi}(i) = \bar{i}$. The number of anti-excedances of $\tilde{\pi}$ (which we usually denote by a) is equal to the number of values $i \in \{1, \dots, b\}$ such that $\tilde{\pi}(i) < i$ or $\tilde{\pi}(i) = \bar{i}$.

Example 7.9.2. The decorated permutation $\tilde{\pi} = (5, \underline{2}, \bar{3}, 6, 4, 1)$ on $b = 6$ letters (see Figure 7.59) has $a = 3$ anti-excedances, namely, 1, 4, and $\bar{3}$. Indeed, $\tilde{\pi}^{-1}(1) = 6 > 1$, and $\tilde{\pi}^{-1}(4) = 5 > 4$.

Definition 7.9.3. Let $\tilde{\pi}$ be a decorated permutation on b letters with a anti-excedances. The *affinization* of $\tilde{\pi}$ is the map $\tilde{\pi}_{\text{aff}} : \mathbb{Z} \rightarrow \mathbb{Z}$ constructed as follows. For $i \in \{1, \dots, b\}$, we set

$$\tilde{\pi}_{\text{aff}}(i) = \begin{cases} \tilde{\pi}(i) & \text{if } \tilde{\pi}(i) > i, \\ i & \text{if } \tilde{\pi}(i) = \underline{i}, \\ \tilde{\pi}(i) + b & \text{if } \tilde{\pi}(i) < i, \\ i + b & \text{if } \tilde{\pi}(i) = \bar{i}. \end{cases}$$

We then extend $\tilde{\pi}_{\text{aff}}$ to \mathbb{Z} so that it satisfies

$$(7.9.1) \quad \tilde{\pi}_{\text{aff}}(i + b) = \tilde{\pi}_{\text{aff}}(i) + b \quad (i \in \mathbb{Z}).$$

We note that

$$(7.9.2) \quad i \leq \tilde{\pi}_{\text{aff}}(i) \leq i + b \quad (i \in \mathbb{Z})$$

and

$$(7.9.3) \quad \sum_{i=1}^b (\tilde{\pi}_{\text{aff}}(i) - i) = b \cdot \#\{i \in \{1, \dots, b\} \mid \tilde{\pi}(i) < i \text{ or } \tilde{\pi}(i) = \bar{i}\} = ab.$$

Example 7.9.4. Continuing with $\tilde{\pi} = (5, \underline{2}, \bar{3}, 6, 4, 1)$ from Example 7.9.2, we get $\tilde{\pi}_{\text{aff}}(1) = 5$, $\tilde{\pi}_{\text{aff}}(2) = 2$, $\tilde{\pi}_{\text{aff}}(3) = 9$, $\tilde{\pi}_{\text{aff}}(4) = 6$, $\tilde{\pi}_{\text{aff}}(5) = 10$, $\tilde{\pi}_{\text{aff}}(6) = 7$, or more succinctly,

$$\tilde{\pi}_{\text{aff}} = (\dots, 5, 2, 9, 6, 10, 7, \dots) = (\dots \boxed{5 \ 2 \ 9 \ 6 \ 10 \ 7} \ 11 \ 8 \ 15 \ 12 \ 16 \ 13 \ \dots).$$

(The boxed terms are the values at $1, \dots, b$. They determine the rest of the sequence by virtue of (7.9.1).) In accordance with (7.9.3), we have

$$(5 + 2 + 9 + 6 + 10 + 7) - (1 + \dots + 6) = 39 - 21 = 18 = 3 \cdot 6 = ab.$$

With the above construction in mind, we introduce the following notion.

Definition 7.9.5. Let a and b be positive integers. An (a, b) -bounded affine permutation is a bijection $f : \mathbb{Z} \rightarrow \mathbb{Z}$ satisfying the following conditions:

- $f(i + b) = f(i) + b$ for all $i \in \mathbb{Z}$;
- $i \leq f(i) \leq i + b$ for all $i \in \mathbb{Z}$;
- $\sum_{i=1}^b (f(i) - i) = ab$.

Lemma 7.9.6. [15] *The correspondence $\tilde{\pi} \mapsto \tilde{\pi}_{\text{aff}}$ described in Definition 7.9.3 restricts to a bijection between decorated permutations on b letters with a anti-excedances and the (a, b) -bounded affine permutations.*

Proof. If $\tilde{\pi}$ is a decorated permutation on b letters with a anti-excedances, then (7.9.1)–(7.9.3) show that $\tilde{\pi}_{\text{aff}}$ is an (a, b) -bounded affine permutation.

Conversely, given an (a, b) -bounded affine permutation $f : \mathbb{Z} \rightarrow \mathbb{Z}$, we can define the decorated permutation $\tilde{\pi}$ on b letters by

$$\tilde{\pi}(i) = \begin{cases} \underline{i} & \text{if } f(i) = i; \\ \bar{i} & \text{if } f(i) = i + b; \\ f(i) & \text{if } f(i) \leq b \text{ and } f(i) \neq i; \\ f(i) - b & \text{if } f(i) > b \text{ and } f(i) \neq i + b. \end{cases}$$

We claim that $\tilde{\pi}$ has a anti-excedances. Using the inequality $i \leq f(i) \leq i + b$, we conclude that the anti-excedances of $\tilde{\pi}$ are in bijection with the values $i \in \{1, \dots, b\}$ such that $f(i) > b$. The claim follows from the observation that $ab = \sum_{i=1}^b (f(i) - i) = b \cdot \#\{i \in \{1, \dots, b\} \mid f(i) > b\}$. \square

Lemma 7.9.6 is illustrated in Figure 7.50 (the first two columns).

| $\tilde{\pi}$ | $\tilde{\pi}_{\text{aff}}$ | $\ell(\tilde{\pi}_{\text{aff}})$ |
|---------------------------------------|---|----------------------------------|
| $\bar{1} \underline{2} \underline{3}$ | $\dots \boxed{4 \ 2 \ 3} \ 7 \ 5 \ 6 \ \dots$ | 2 |
| $\underline{1} \bar{2} \underline{3}$ | $\dots \boxed{1 \ 5 \ 3} \ 4 \ 8 \ 6 \ \dots$ | 2 |
| $\underline{1} \underline{2} \bar{3}$ | $\dots \boxed{1 \ 2 \ 6} \ 4 \ 5 \ 9 \ \dots$ | 2 |
| $2 \ 1 \underline{3}$ | $\dots \boxed{2 \ 4 \ 3} \ 5 \ 7 \ 6 \ \dots$ | 1 |
| $\underline{1} \ 3 \ 2$ | $\dots \boxed{1 \ 3 \ 5} \ 4 \ 6 \ 8 \ \dots$ | 1 |
| $3 \underline{2} \ 1$ | $\dots \boxed{3 \ 2 \ 4} \ 6 \ 5 \ 7 \ \dots$ | 1 |
| $2 \ 3 \ 1$ | $\dots \boxed{2 \ 3 \ 4} \ 5 \ 6 \ 7 \ \dots$ | 0 |

Figure 7.50. Decorated permutations $\tilde{\pi}$ on $b=3$ letters with $a=1$ anti-excedance; the corresponding (a, b) -bounded affine permutations $\tilde{\pi}_{\text{aff}}$; and the lengths $\ell(\tilde{\pi}_{\text{aff}})$ of these affine permutations.

Recall from Exercise 7.4.21 that the number of decorated permutations on b letters is equal to $b! \sum_{k=0}^b \frac{1}{k!}$. The following result, stated here without proof, refines this count by taking into account the number of anti-excedances.

Proposition 7.9.7 ([25, Theorem 4.1], [21, Proposition 23.1]). *Let $D_{a,b}$ be the number of decorated permutations on b letters with a anti-excedances (or the number of (a, b) -bounded affine permutations, cf. Lemma 7.9.6). Then*

$$D_{a,b} = \sum_{i=0}^{a-1} (-1)^i \binom{b}{i} ((a-i)^i (a-i+1)^{b-i} - (a-i-1)^i (a-i)^{b-i}),$$

$$\sum_{0 \leq a \leq b} D_{a,b} x^a \frac{y^b}{b!} = e^{xy} \frac{x-1}{x - e^{y(x-1)}}.$$

Definition 7.9.8. Let $\tilde{\pi}_{\text{aff}}$ be an (a, b) -bounded affine permutation, an affinization of a decorated permutation $\tilde{\pi}$, cf. Lemma 7.9.6. We refer to a position $i \in \mathbb{Z}$ such that $\tilde{\pi}_{\text{aff}}(i) \equiv i \pmod{b}$ (in other words, $\tilde{\pi}_{\text{aff}}(i) \in \{i, i+b\}$; and if $1 \leq i \leq b$ then $\tilde{\pi}(i) \in \{\underline{i}, \bar{i}\}$) as a *fixed point* of $\tilde{\pi}_{\text{aff}}$. If every $i \in \mathbb{Z}$ is a fixed point of $\tilde{\pi}_{\text{aff}}$, then we say that $\tilde{\pi}_{\text{aff}}$ is *equivalent to the identity modulo b* (or that $\tilde{\pi}$ is a decoration of the identity).

Lemma 7.9.9. *If $\tilde{\pi}_{\text{aff}}$ is not equivalent to the identity modulo b , then there exist $i, j \in \mathbb{Z}$ such that*

$$(7.9.4) \quad 1 \leq i < j \leq b,$$

$$(7.9.5) \quad \tilde{\pi}_{\text{aff}}(i) < \tilde{\pi}_{\text{aff}}(j),$$

$$(7.9.6) \quad \text{every position } h \text{ such that } i < h < j \text{ is a fixed point of } \tilde{\pi}_{\text{aff}}, \text{ and}$$

$$(7.9.7) \quad \text{neither } i \text{ nor } j \text{ are fixed points of } \tilde{\pi}_{\text{aff}}.$$

Proof. Suppose such a pair (i, j) does not exist. Let $i_1 < \dots < i_m$ be the elements of $\{1, \dots, b\}$ that are not fixed points of $\tilde{\pi}_{\text{aff}}$. Then

$$i_1 < \dots < i_m < \tilde{\pi}_{\text{aff}}(i_m) \leq \dots \leq \tilde{\pi}_{\text{aff}}(i_1).$$

We conclude that none of the values $\tilde{\pi}_{\text{aff}}(i_j)$ is of the form i_ℓ and consequently is of the form $i_\ell + b$. In particular, $\tilde{\pi}_{\text{aff}}(i_j) = i_m + b$ for some $j \neq m$. This implies $\tilde{\pi}_{\text{aff}}(i_j) > i_j + b$, a contradiction. \square

Definition 7.9.10. An *inversion* of $\tilde{\pi}_{\text{aff}}$ is a pair of integers (i, j) such that $i < j$ and $\tilde{\pi}_{\text{aff}}(i) > \tilde{\pi}_{\text{aff}}(j)$. Two inversions (i, j) and (i', j') are *equivalent* if $i' - i = j' - j \in b\mathbb{Z}$. The *length* $\ell(\tilde{\pi}_{\text{aff}})$ of $\tilde{\pi}_{\text{aff}}$ is the number of equivalence classes of inversions. (These classes correspond to the *alignments* of $\tilde{\pi}$, as defined in [21].) This number is finite since for any inversion (i, j) , we have $i < j < i + b$. Indeed, if $j \geq i + b$, then $\tilde{\pi}_{\text{aff}}(j) \geq j \geq i + b \geq \tilde{\pi}_{\text{aff}}(i)$. See Figure 7.50.

Lemma 7.9.11. *Let $\tilde{\pi}_{\text{aff}}$ be an (a, b) -bounded affine permutation that is equivalent to the identity modulo b . Then $\ell(\tilde{\pi}_{\text{aff}}) = a(b - a)$.*

Proof. Let $I = \{i \in \{1, \dots, b\} \mid \tilde{\pi}_{\text{aff}}(i) = i + b\}$ and $\underline{I} = \{i \in \{1, \dots, b\} \mid \tilde{\pi}_{\text{aff}}(i) = i\}$. Then $|I| = a$ and $|\underline{I}| = b - a$. The equivalence classes of inversions of $\tilde{\pi}_{\text{aff}}$ are described by the following list of representatives:

$$\{(i, j) \in I \times \underline{I} \mid 1 \leq i < j \leq b\} \cup \{(i, j + b) \mid (i, j) \in I \times \underline{I}, 1 \leq j < i \leq b\}.$$

The cardinality $\ell(\tilde{\pi}_{\text{aff}})$ of this set is equal to $|I \times \underline{I}| = a(b - a)$. \square

We next describe an algorithm for factoring affine permutations.

Definition 7.9.12. Let $\tilde{\pi}_{\text{aff}}$ be an (a, b) -bounded affine permutation. If $\tilde{\pi}_{\text{aff}}$ is not equivalent to the identity modulo b , then by Lemma 7.9.9, there exist positions $i, j \in \mathbb{Z}$ satisfying (7.9.4)–(7.9.7). We then swap the values of $\tilde{\pi}_{\text{aff}}$ in positions i and j (and more generally, in positions $i + mb$ and $j + mb$, for all $m \in \mathbb{Z}$). We repeat this procedure until we obtain an affine permutation that is equivalent to the identity modulo b . The algorithm terminates because each swap increases the length of the affine permutation by 1; this number is bounded by Definition 7.9.10. See Figure 7.51.

| (i, j) | 1 | 2 | 3 | 4 | 5 | 6 |
|----------|---|---|---|---|---|---|
| (34) | 4 | 6 | 5 | 7 | 8 | 9 |
| (23) | 4 | 6 | 7 | 5 | 8 | 9 |
| (12) | 4 | 7 | 6 | 5 | 8 | 9 |
| (56) | 7 | 4 | 6 | 5 | 8 | 9 |
| (45) | 7 | 4 | 6 | 5 | 9 | 8 |
| (34) | 7 | 4 | 6 | 9 | 5 | 8 |
| (46) | 7 | 4 | 9 | 6 | 5 | 8 |
| (24) | 7 | 4 | 9 | 8 | 5 | 6 |
| | 7 | 8 | 9 | 4 | 5 | 6 |

Figure 7.51. Factoring $\tilde{\pi}_{\text{aff}} = (4, 6, 5, 7, 8, 9)$. The entries corresponding to the fixed points of $\tilde{\pi}_{\text{aff}}$ are boxed. Here $\tilde{\pi} = (4, 6, 5, 1, 2, 3)$.

Remark 7.9.13. In view of (7.9.3), the affine permutation at hand remains (a, b) -bounded after each step of the algorithm in Definition 7.9.12. It then follows from Lemma 7.9.11 that among all (a, b) -bounded affine permutations $\tilde{\pi}_{\text{aff}}$, the ones that have the maximal possible length $\ell(\tilde{\pi}_{\text{aff}}) = a(b - a)$ are precisely the ones that are equivalent to the identity modulo b .

7.10. Bridge decompositions

Bridge decompositions [2, Section 3.2] provide a useful recursive construction of reduced plabic graphs with a given decorated trip permutation.

Definition 7.10.1. A *bridge* is a graph fragment shown in Figure 7.52 on the left. Let $\tilde{\pi}$ be a decorated permutation on b letters that has a anti-excedances, and let $\tilde{\pi}_{\text{aff}}$ be the corresponding affine permutation. To build a plabic graph associated to $\tilde{\pi}_{\text{aff}}$, we begin by introducing a white (resp., black) lollipop in each position i with $\tilde{\pi}(i) = \bar{i}$ (resp., $\tilde{\pi}(i) = \underline{i}$). If $\tilde{\pi}$ is a decoration of the identity, we are done. Otherwise, we generate a sequence of transpositions (i, j) following the algorithm in Definition 7.9.12, then attach successive bridges in the corresponding positions, as in Figure 7.52. The resulting graph is called a *bridge decomposition* of $\tilde{\pi}_{\text{aff}}$, or sometimes a BCFW bridge decomposition, due to its relation with the Britto-Cachazo-Feng-Witten recursion in quantum field theory, see [2].

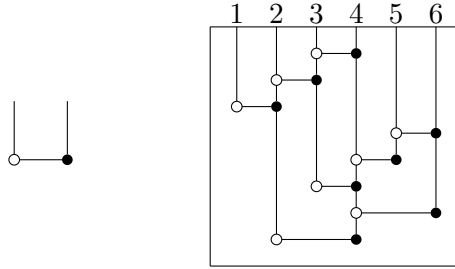


Figure 7.52. *Left:* a single bridge. *Right:* the bridge decomposition associated to the factorization constructed in Figure 7.51. The resulting plabic graph has trip permutation $\tilde{\pi} = (4, 6, 5, 1, 2, 3)$. Moreover, we have $\tilde{\pi} = (24)(46)(34)(45)(56)(12)(23)(34)$, the product of the transpositions (i, j) generated by the algorithm (reading right to left).

Proposition 7.10.2. A bridge decomposition of an (a, b) -bounded affine permutation $\tilde{\pi}_{\text{aff}}$ uses $a(b - a) - \ell(\tilde{\pi}_{\text{aff}})$ bridges.

Proof. See Lemma 7.9.11 and Definitions 7.9.12 and 7.10.1. \square

Theorem 7.10.3. Let $\tilde{\pi}$ be a decorated permutation on b letters that has a anti-excedances. Let $\tilde{\pi}_{\text{aff}}$ be the associated (a, b) -bounded affine permutation. Then any bridge decomposition of $\tilde{\pi}_{\text{aff}}$ is a reduced plabic graph with the decorated trip permutation $\tilde{\pi}$.

Proof. We use induction on the number of bridges $\beta = a(b - a) - \ell(\tilde{\pi}_{\text{aff}})$. If $\beta = 0$, then $\tilde{\pi}$ is a decoration of the identity (see Remark 7.9.13), so the bridge decomposition consists entirely of lollipops, and we are done.

Now suppose that $\tilde{\pi}$ is not a decoration of the identity. Proceeding as in Definition 7.9.12, we construct a sequence of transpositions $\sigma_1, \sigma_2, \dots, \sigma_\beta$,

where $\sigma_1 = (ij)$ satisfies (7.9.4)–(7.9.7). Let G be the plabic graph obtained by attaching bridges according to $\sigma_1, \dots, \sigma_\beta$ (from top to bottom). By the induction assumption, attaching bridges according to $\sigma_2, \dots, \sigma_\beta$ as in Definition 7.10.1 produces a reduced plabic graph G' with the trip permutation $\tilde{\pi}' = \sigma_\beta \cdots \sigma_2$. This graph has $\beta - 1$ bridges and is obtained by removing the topmost horizontal edge e from G and applying local moves (M2) to remove the endpoints of e .

Conversely, G is obtained from G' by attaching a bridge in position (i, j) at the top of G' . (To illustrate, in Figure 7.52 we have $(i, j) = (3, 4)$.) When we add this bridge to G' , the trips starting at i and j get their “tails” swapped: the trip T_i (resp., T_j) in G that begins at i (resp., at j) traverses e and continues along the trip that used to begin at j (resp., at i) in G' ; all other trips remain the same. Hence the trip permutation of G is $\tilde{\pi}'\sigma_1 = \tilde{\pi}$.

It remains to show that G is reduced. It is tempting to try to use for this purpose the “bad features” criterion of Theorem 7.8.6. However, this theorem requires the plabic graph to be normal, so we will need to replace G by a suitable normal graph $N(G)$. It will also be more convenient to utilize the triple diagram version of the criterion, cf. Corollary 7.8.5.

We begin by constructing the normal graph $N(G)$ using Definition 7.8.2. (Note that stages 1, 4 and 6 of the algorithm are not needed since every vertex in G has degree 2 or 3, or is a lollipop that gets removed.) Up to the addition/removal of lollipops, the triple diagram $\mathfrak{X}(N(G))$ is isotopic to the triple diagram $\mathfrak{X}(G)$ constructed directly from G as in Definition 7.5.17. The graph G is reduced if and only if $N(G)$ is reduced, which is equivalent to the triple diagram $\mathfrak{X} = \mathfrak{X}(N(G)) = \mathfrak{X}(G)$ being minimal, or to \mathfrak{X} having no badgons, see Corollary 7.8.5. Thus, our goal is to show \mathfrak{X} has no badgons.

By the induction assumption, the triple diagram $\mathfrak{X}' = \mathfrak{X}(G')$ has no badgons. It follows that any potential badgon in \mathfrak{X} must involve the white endpoint w of edge e ; otherwise this feature would have already been present in \mathfrak{X}' . In particular, this means that w is trivalent, i.e., not an elbow of G .

A monogon in \mathfrak{X} would have to have its vertex at w . Three of the six half-strands at w run straight to or from the boundary, so we need to use two of the remaining three; moreover, those two half-strands have to be oppositely oriented. There are two such cases to consider. In one case, i would be a fixed point of $\tilde{\pi}$, contradicting our choice of (i, j) . In the other case, i would be a fixed point of $\tilde{\pi}' = \tilde{\pi}(G')$, which can also be ruled out since in that case, i would not participate in any bridge in G' , making it impossible to produce the bottom vertex of the vertical edge pointing downwards from w .

Finally, suppose that \mathfrak{X} contains a parallel digon. One of the vertices of the digon has to be w ; let w' denote the other vertex. Since the two sides of the digon are oriented in the same way at w , it follows that these sides lie on the strands S_i and S_j that start near the vertices i and j , respectively.

By our choice of bridge (i, j) , every h with $i < h < j$ is a fixed point of $\tilde{\pi}$, but i and j are not fixed points. It follows that S_i (resp. S_j) does not terminate at i (resp. j), and neither terminates between the boundary vertices i and j . We explained in the monogon case that S_j cannot terminate at i ; one can similarly argue that S_i cannot terminate at j . Also, neither S_i nor S_j intersects itself. Moreover the “tails” of S_i and S_j that start at the second vertex w' of the digon do not intersect each other (since otherwise a parallel digon would have been present in \mathfrak{X}'). It follows that either $\tilde{\pi}(i) < i$ and $\tilde{\pi}(j) > j$, or $\tilde{\pi}(i) > \tilde{\pi}(j) > j$, or $\tilde{\pi}(j) < \tilde{\pi}(i) < i$. In each case, we get $\tilde{\pi}_{\text{aff}}(i) > \tilde{\pi}_{\text{aff}}(j)$, which contradicts the way we chose i and j . \square

Corollary 7.10.4. *Let $\tilde{\pi}$ be a decorated permutation on b letters. Then there exists a reduced plabic graph whose decorated trip permutation is $\tilde{\pi}$.*

Proof. Use either Theorem 7.10.3 or the construction in Definition 7.6.8 (together with Proposition 7.5.12 and Theorem 7.7.3). \square

Corollary 7.10.5. *Let G be a reduced plabic graph with the decorated trip permutation $\tilde{\pi}$. If $\tilde{\pi}$ has b letters and a anti-excedances, then the number of faces in G is $a(b - a) - \ell(\tilde{\pi}_{\text{aff}}) + 1$.*

Proof. The number of faces is invariant under local moves. Therefore, by Theorem 7.4.25, it suffices to establish this formula for a particular reduced plabic graph with decorated trip permutation $\tilde{\pi}$. By Theorem 7.10.3, we can use a bridge decomposition of $\tilde{\pi}_{\text{aff}}$. Since each bridge adds one face to the graph, the claim follows by Proposition 7.10.2. \square

Let $\tilde{\pi}_{a,b}$ denote the decorated permutation on b letters defined by

$$(7.10.1) \quad \tilde{\pi}_{a,b} = (a + 1, a + 2, \dots, b, 1, 2, \dots, a).$$

Exercise 7.10.6. Let $\tilde{\pi}$ be a decorated permutation on b letters that has a anti-excedances. Show that if $\ell(\tilde{\pi}_{\text{aff}}) = 0$, then $\tilde{\pi} = \tilde{\pi}_{a,b}$.

Corollary 7.10.7. *Let G be a reduced plabic graph whose decorated trip permutation $\tilde{\pi}_G$ has b letters and a anti-excedances. Then G has at most $a(b - a) + 1$ faces. Moreover it has $a(b - a) + 1$ faces if and only if $\tilde{\pi}_G = \tilde{\pi}_{a,b}$.*

Proof. Immediate from Corollary 7.10.5 and Exercise 7.10.6. \square

Remark 7.10.8. The *permutohedron* \mathcal{P}_n [23, Exercise 4.64a] is a polytope whose $n!$ vertices are labeled by permutations in the symmetric group \mathcal{S}_n . Shortest paths in the 1-skeleton of \mathcal{P}_n encode reduced expressions in \mathcal{S}_n , and its 2-dimensional faces correspond to their local (braid) transformations, cf. Exercise 7.4.7. Similarly, paths in the 1-skeleton of the *bridge polytope* [26] encode bridge decompositions of the decorated permutation $\tilde{\pi}_{a,b}$; its 2-dimensional faces correspond to local moves in plabic graphs.

7.11. Edge labels of reduced plabic graphs

Definition 7.11.1. Let G be a plabic graph. Let us label the edges of G by subsets of integers that indicate which one-way trips traverse a given edge; more precisely, for each boundary vertex i , we include i in the label of every edge contained in the trip that starts at i . By Remark 7.4.15, each edge will be labeled by at most two integers. See Figure 7.53.

We say that G has the *resonance property* if after labeling the edges of G as in Definition 7.11.1, the following condition is satisfied at each internal vertex v that is not a lollipop:

- there exist numbers $i_1 < \dots < i_m$ such that the edges incident to v are labeled by the two-element sets $\{i_1, i_2\}, \{i_2, i_3\}, \dots, \{i_{m-1}, i_m\}, \{i_1, i_m\}$, appearing in clockwise order.

In particular, each edge of G that is not incident to a lollipop is labeled by a two-element subset. See Figure 7.53.

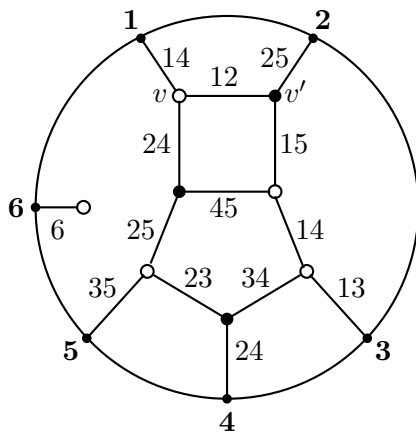


Figure 7.53. A reduced plabic graph from Figures 7.1(b) and 7.21. Its edge labeling exhibits the resonance property, see Definition 7.11.1. For example, the edge labels around the vertex v (resp., v'), listed in clockwise order, are $\{1, 2\}, \{2, 4\}, \{1, 4\}$ (resp., $\{1, 2\}, \{2, 5\}, \{1, 5\}$).

Remark 7.11.2. If a plabic graph has an internal leaf that is not a lollipop, then the resonance property fails. At a bivalent vertex v , the resonance condition is satisfied if and only if the two trips passing through v are distinct and none of them is a roundtrip.

Remark 7.11.3. If a plabic graph G is trivalent (apart from lollipops), then the resonance property is equivalent to the following requirement at each interior vertex v (other than a lollipop):

- the three edges incident to v have labels $\{a, b\}, \{a, c\}$, and $\{b, c\}$, for some $a < b < c$, and moreover this (lexicographic) ordering of labels corresponds to the counterclockwise direction around v .

For example, in Figure 7.53, the edge labels around the vertex v (resp., v') are, in lexicographic order, $\{1, 2\}, \{1, 4\}, \{2, 4\}$ (resp., $\{1, 2\}, \{1, 5\}, \{2, 5\}$). The three edges carrying these labels appear in the counterclockwise order around v (resp., v').

Exercise 7.11.4. Verify that none of the plabic graphs shown in Figure 7.48 (draw a disk around each of the fragments) satisfy the resonance property.

Theorem 7.11.5 ([16, Theorem 10.5]). *Let G be a plabic graph without internal leaves other than lollipops. Then G is reduced if and only if it has the resonance property.*

Theorem 7.11.5 is proved below in this section, following a few remarks and auxiliary lemmas.

Remark 7.11.6. Theorem 7.11.5 can be used to test whether a given plabic graph (potentially having internal leaves) is reduced or not. To this end, use the moves (M2) and (M3) to get rid of collapsible trees. If an internal leaf (not a lollipop) remains, then the graph is not reduced. Otherwise, one can apply the criterion in Theorem 7.11.5.

Remark 7.11.7. We find the resonance criterion of Theorem 7.11.5 easier to check than the “bad features” criterion of Theorem 7.8.6.

Remark 7.11.8. Certain reduced plabic graphs were realized as tropical curves in [16], where it was shown that the resonance property corresponds to the *balancing condition* for tropical curves.

Lemma 7.11.9. *The resonance property is preserved under the local moves (M1)–(M3), except when the decontraction move (M3) creates a new leaf.*

Proof. The square move (M1) only changes the labels of the sides of the square, see Figure 7.54. Moreover, the labels around each vertex match the labels around the opposite vertex after the square move, with the same cyclic order. Hence this move preserves the resonance property.

The case of the local move (M2) is easy, cf. Remark 7.11.2.

For the case of the local move (M3), see Figure 7.55. □

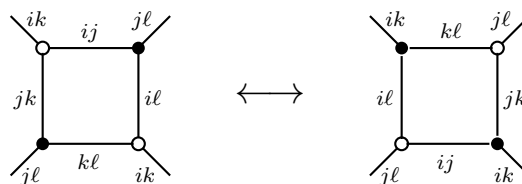


Figure 7.54. Transformation of edge labels under a square move (M1).

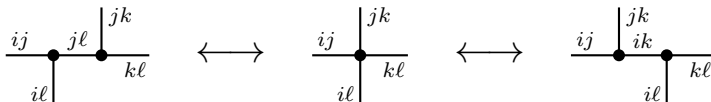


Figure 7.55. Transformation of edge labels under a local move (M3) at a 4-valent black vertex. (Alternatively, make all the vertices white.)

Lemma 7.11.10. *Any plabic graph obtained via the bridge decomposition construction (see Definition 7.10.1) has the resonance property.*

Proof. We will show that, more concretely, the edge labels around trivalent vertices in such a plabic graph G follow one of the patterns described in Figure 7.56. We will establish this result by induction on β , the number of bridges, following the strategy used in the proof of Theorem 7.10.3.

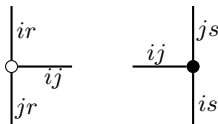


Figure 7.56. Edge labels near trivalent vertices in a bridge decomposition. At a white vertex, shown on the left, either $r < i < j$ or $i < j < r$. At a black vertex, shown on the right, either $s < i < j$ or $i < j < s$.

Let G be a bridge decomposition of $\tilde{\pi}_{\text{aff}}$, associated to the sequence of transpositions $\sigma_1, \dots, \sigma_\beta$. Thus $\tilde{\pi} = \tilde{\pi}_G = \sigma_\beta \cdots \sigma_1$. Here $\sigma_1 = (ij)$, where i and j satisfy (7.9.4)–(7.9.7). Let G' be the bridge decomposition associated to $\sigma_2, \dots, \sigma_\beta$, so that G is obtained from G' by adding a single bridge in position (i, j) at the top of G' .

Suppose the result is true for G' . We need to verify it for G . Let $r = \tilde{\pi}^{-1}(i)$ and $s = \tilde{\pi}^{-1}(j)$. Adding the bridge in position (i, j) at the top of G' adds at most two trivalent vertices: it adds a white (respectively, black) trivalent vertex provided that $r \neq j$ (respectively, $s \neq i$). The cases when one of the vertices on the bridge is bivalent are easy to verify, so we are going to assume that $r \neq j$ and $s \neq i$. In this case, the local configuration around positions i and j in G' and G is as shown in Figure 7.57.

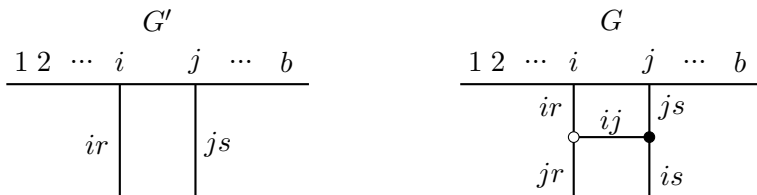


Figure 7.57. The local configuration around positions i and j in G' and G .

Recall that $i < j$ and moreover any h such that $i < h < j$ is a fixed point of $\tilde{\pi}$. For the reasons indicated in the proof of Theorem 7.10.3, adding the bridge (i, j) at the top of G' has the effect of replacing the label i (resp., j) by j (resp., i) in every edge label outside of the bridge.

If G' has an edge with the label ij , then G has a bad double crossing involving the trips originating at i and j . This however is impossible since G is reduced, by Theorem 7.10.3. Therefore G' has no edge with label ij . Furthermore, G' has no edge with a label h for $i < h < j$. Since all trivalent vertices of G' satisfy the resonance condition of Figure 7.56, the same remains true after switching the labels i and j . Thus, all trivalent vertices of G that were present in G' satisfy this resonance condition.

Finally, the two new trivalent vertices in G satisfy this condition because $i < j$ and we can exclude $i < r < j$ and $i < s < j$ because of (7.9.6). \square

Proof of Theorem 7.11.5. We first establish the “if” direction. Let G be a plabic graph without internal leaves that are not lollipops. Suppose that G has the resonance property. We want to show that G is reduced.

Assume the contrary. By Proposition 7.4.9, G can be transformed by local moves that don’t create internal leaves into a plabic graph G' containing a hollow digon. Since G has the resonance property, so does G' , by Lemma 7.11.9. This yields a contradiction because the labels around a hollow digon do not satisfy the resonance property, see Figure 7.58.

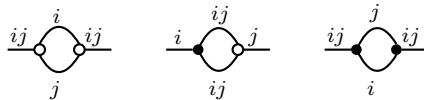


Figure 7.58. A plabic graph containing a hollow digon fails to satisfy the resonance property.

We next establish the “only if” direction. Suppose that G is reduced, with $\tilde{\pi}_G = \tilde{\pi}$. We know from Theorem 7.10.3 that there is a bridge decomposition G' —a reduced plabic graph—with trip permutation $\tilde{\pi}$. By Lemma 7.11.10, G' has the resonance property. By Theorem 7.4.25, $G \sim G'$.

Since G has no internal leaves, there exists a trivalent plabic graph $G_3 \sim G$, see Lemma 7.3.2. Moreover it can be seen from the proof of this lemma that G and G_3 are related via moves that do not create internal leaves, so by Lemma 7.11.9 G has the resonance property if and only if G_3 does. Similarly, by removing bivalent vertices from G' , we obtain a trivalent graph $G'_3 \sim G'$ that has the resonance property. Since G_3 and G'_3 are trivalent and move-equivalent to each other, they are related via a sequence of (M1) and (M4) moves, see Theorem 7.3.5. By Lemma 7.11.9, these local moves preserve the resonance property, so G_3 has the resonance property and therefore G has it as well. \square

7.12. Face labels of reduced plabic graphs

In this section, we use the notion of a trip introduced in Definition 7.4.12 to label each face of a reduced plabic graph by a collection of positive integers. These face labels generalize the labeling of diagonals in a polygon by Plücker coordinates (cf. Section 1.2) as well as the labeling of faces in (double or ordinary) wiring diagrams by chamber minors (cf. Sections 1.3–1.4). In the following chapter, we will relate the face labels of reduced plabic graphs to Plücker coordinates that form an extended cluster for the standard cluster structure on a Grassmannian or, more generally, on a Schubert or positroid subvariety within it.

Remark 7.12.1. Let G be a reduced plabic graph. Let T_i be the one-way trip in G that begins at a boundary vertex i and ends at a boundary vertex j .

If $i \neq j$, then we claim that there are two kinds of faces in G : those on the left side of the trip T_i and those on the right side of it. If G is normal, then this claim follows from the fact (see Theorem 7.8.6) that G does not contain essential self-intersections. For a general reduced plabic graph, the claim can be deduced from the case of normal graphs using the procedure described in Definition 7.8.2.

If $i = j$, then by Proposition 7.4.22, the boundary vertex i is the root of a tree that collapses to a lollipop. If this lollipop is white (resp., black), then we declare that all faces of G lie on the left (resp., right) side of the trip T_i .

Definition 7.12.2. Let G be a reduced plabic graph with boundary vertices $1, \dots, b$. We define two natural face labelings of G , cf. Figure 7.59:

- in the *source labeling* $\mathcal{F}_{\text{source}}(G)$, each face f of G is labeled by the set

$$I_{\text{source}}(f) = \{i \mid f \text{ lies to the left of the trip starting at vertex } i\};$$

- in the *target labeling* $\mathcal{F}_{\text{target}}(G)$, each face f of G is labeled by the set

$$I_{\text{target}}(f) = \{i \mid f \text{ is to the left of the trip ending at vertex } i\}.$$

Remark 7.12.3. The edge labeling and the face labeling of a reduced plabic graph G are related as follows: if two faces f and f' of G are separated by a single edge whose edge label is $\{i, j\}$, then the face label of f' is obtained from that of f by either removing i and adding j , or removing j and adding i .

Theorem 7.12.4. Let G be a reduced plabic graph with b boundary vertices. Let a denote the number of anti-excedances in the trip permutation π_G . Let us label the faces of G using either the source or the target labeling. Then every face of G will be labeled by an a -element subset of $\{1, \dots, b\}$.

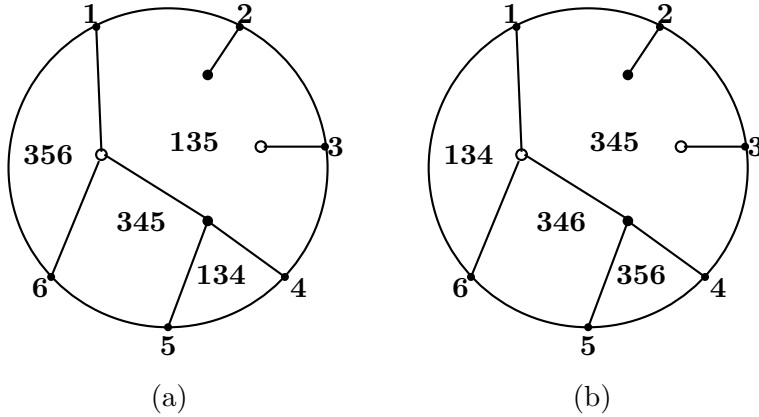


Figure 7.59. (a) The source labeling $\mathcal{F}_{\text{source}}(G)$ of a reduced plabic graph G . (b) The target labeling $\mathcal{F}_{\text{target}}(G)$. Here $\tilde{\pi}_G = (5, \underline{2}, \bar{3}, 6, 4, 1)$. Every face is labeled by a subset of cardinality 3, in agreement with Theorem 7.12.4, cf. Example 7.9.2.

Proof. By Theorem 7.11.5, every reduced plabic graph G has the resonance property, which in particular means that every edge label of G consists of two distinct numbers. It then follows from Remark 7.12.3 that every face label of G has the same cardinality. It remains to show that this cardinality is a , the number of anti-excedances of $\tilde{\pi} = \tilde{\pi}_G$.

Furthermore, it is sufficient to establish the latter claim for one particular reduced plabic graph with the trip permutation $\tilde{\pi}_G$, e.g., for a bridge decomposition of $\tilde{\pi}_{\text{aff}}$. Indeed, any two reduced plabic graphs with the same trip permutation are related by local moves, and any such move preserves all labels except at most one, see Exercise 7.12.5.

To prove the theorem for bridge decompositions, we use induction on the number of bridges β . In the base case $\beta = 0$, the bridge decomposition G consists of a white lollipops, $b - a$ black lollipops, and no bridges. Thus G has a single face, labeled by the a -element subset indicating the positions of the white lollipops.

Consider a bridge decomposition G built from a bridge decomposition G' by adding a bridge in position (i, j) at the top of G' , as in Figure 7.57. Both G and G' have trip permutations with a anti-excedances (cf. Remark 7.9.13), so by the induction assumption, the faces in G' have cardinality a . Since G inherits most of its faces from G' , and all face labels of G have the same cardinality, this cardinality is equal to a . \square

Exercise 7.12.5. Verify that applying a move (M2) or (M3) does not affect the face labels of a plabic graph, whereas applying the square move (M1) changes the face labels as shown in Figure 7.60.

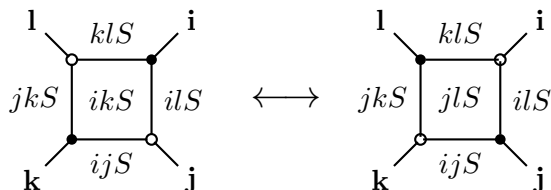


Figure 7.60. The effect of the square move (M1) on the face labeling. Here i, j, k, l are the (source or target) labels of the trips that traverse the outer edges towards the central square; S is an arbitrary set of labels disjoint from $\{i, j, k, l\}$; and abS is a shorthand for the set $\{a, b\} \cup S$.

The face labelings of plabic graphs can be used to recover the labelings of diagonals in a polygon by Plücker coordinates as well as the labelings of chambers in (ordinary or double) wiring diagrams by minors:

Exercise 7.12.6. Let T be a triangulation of a convex m -gon \mathbf{P}_m , and let $G(T)$ be the plabic graph defined in Example 7.2.1. Explain how to label the boundary vertices of $G(T)$ in such a way that the face labeling of $G(T)$ recovers the labeling of diagonals of \mathbf{P}_m by pairs of integers. Cf. Figure 7.61.

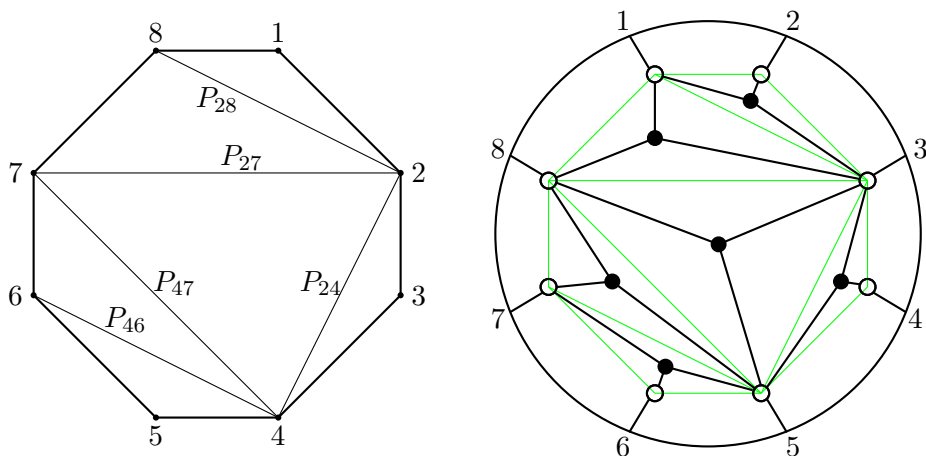


Figure 7.61. A triangulation T of an octagon and the corresponding plabic graph $G(T)$, cf. Figure 2.2.

Exercise 7.12.7. Let D be a wiring diagram with m wires. Let $G(D)$ be the plabic graph defined in Example 7.2.4, see also Figure 7.62. Label the boundary vertices of $G(D)$ by the numbers $1, \dots, 2m$ in the clockwise order, starting with a 1 at the lower left boundary vertex of $G(D)$. Label the faces of $G(D)$ using the source labeling $\mathcal{F}_{\text{source}}(G)$. Show that intersecting each face label with the set $\{1, 2, \dots, m\}$ recovers the labeling of D by chamber minors. See Figure 7.62.

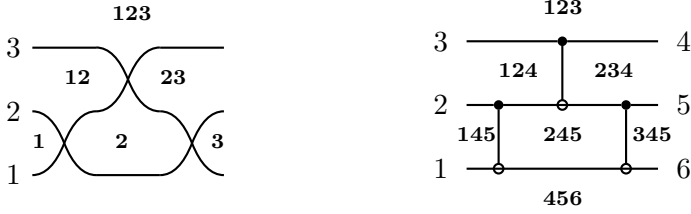


Figure 7.62. A wiring diagram D and the plabic graph $G(D)$ with the source labeling of its faces.

Exercise 7.12.8. Let D be a double wiring diagram with m pairs of wires. Let $G(D)$ be the plabic graph defined in Example 7.2.8. Label the boundary vertices of $G(D)$ by the numbers

$$1, 2, \dots, m - 1, m, m', \dots, 2', 1'$$

in clockwise order, starting with the label 1 at the lower left boundary vertex of $G(D)$. Label the faces of $G = G(D)$ using the source labeling $\mathcal{F}_{\text{source}}(G)$, so that each face gets labeled by $I' \cup J$, where $I' \subset \{1', \dots, m'\}$ and $J \subset \{1, \dots, m\}$. Let I denote the set obtained from I' by replacing each i' by i . Show that mapping each face label $I' \cup J$ to the pair $([1, m] \setminus I, \mathbf{J})$ recovers the labeling of D by chamber minors. See Figure 7.63.

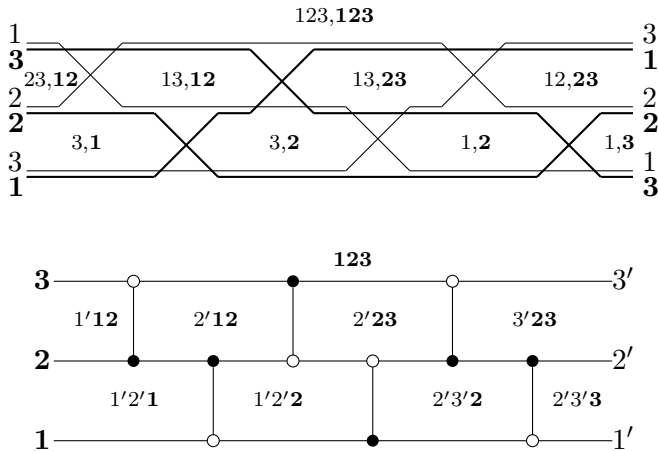


Figure 7.63. Double wiring diagram labeling from plabic graphs. The labeling of a double wiring diagram D is obtained from the source labeling of the associated plabic graph $G(D)$ using the recipe described in Exercise 7.12.8.

7.13. Grassmann necklaces and weakly separated collections

Fix two nonnegative integers b and $a \leq b$. We denote by $\binom{[b]}{a}$ the set of all a -element subsets of $\{1, \dots, b\}$.

In this section, we provide an intrinsic combinatorial characterization of the subsets of $\binom{[b]}{a}$ that arise as sets of face labels of reduced plabic graphs. The proofs are omitted.

Definition 7.13.1 ([18]). We say that two a -element subsets $I, J \in \binom{[b]}{a}$ are *weakly separated* if there do not exist $i, j, i', j' \in \{1, \dots, b\}$ such that

- $i < j < i' < j'$ or $j < i' < j' < i$ or $i' < j' < i < j$ or $j' < i < j < i'$;
- $i, i' \in I \setminus J$ and $j, j' \in J \setminus I$.

Put differently, I and J are weakly separated if and only if, after drawing the numbers $1, 2, \dots, b$ clockwise around a circle, there exists a chord separating the sets $I \setminus J$ and $J \setminus I$ from each other.

Theorem 7.13.2 ([5, 19]). *Let I and J be target face labels of two faces in a reduced plabic graph. Then I and J are weakly separated.*

Definition 7.13.3. A collection $\mathcal{C} \subset \binom{[b]}{a}$ of a -element subsets of $[b]$ is called *weakly separated* if any $I, J \in \mathcal{C}$ are weakly separated. Thus, Theorem 7.13.2 asserts that the collection of target face labels of a reduced plabic graph is weakly separated. A weakly separated collection \mathcal{C} is called *maximal* if it is not contained in any other weakly separated collection. See Figure 7.64.

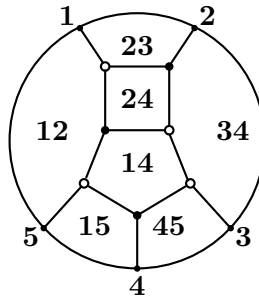


Figure 7.64. The target face labeling of the reduced plabic graph G from Figure 7.1(a). The set of labels $\{12, 23, 34, 45, 15, 24, 14\}$ is a maximal weakly separated collection in $\binom{[5]}{2}$. Here $\tilde{\pi}_G = \tilde{\pi}_{2,5} = (3, 4, 5, 1, 2)$.

Theorem 7.13.4 ([5, 19]). *For $\mathcal{C} \subset \binom{[b]}{a}$, the following are equivalent:*

- \mathcal{C} is a maximal weakly separated collection;
- \mathcal{C} is the set of target face labels of a reduced plabic graph G with $\tilde{\pi}_G = \tilde{\pi}_{a,b}$ (see (7.10.1)).

In that case, the cardinality of \mathcal{C} is equal to $|\mathcal{C}| = a(b - a) + 1$.

Remark 7.13.5. A general formula for the number of maximal weakly separated collections in $\binom{[b]}{a}$ is unknown. For $a = 2$, the maximal weakly separated collections in $\binom{[b]}{2}$ are in bijection with triangulations of a convex b -gon, so they are counted by the Catalan numbers C_{b-2} , where $C_n = \frac{1}{n+1} \binom{2n}{n}$. For $a = 3$ and $b = 6, \dots, 12$, the number of maximal weakly separated collections in $\binom{[b]}{3}$ is equal to 34, 259, 2136, 18600, 168565, 1574298, 15051702. See [6] for more data.

Theorem 7.13.4 can be generalized to arbitrary reduced plabic graphs. To state this result, we will need the following notion.

Definition 7.13.6 ([21, Definition 16.1]). A *Grassmann necklace* of type (a, b) is a sequence $\mathcal{I} = (I_1, \dots, I_b)$ of subsets $I_i \in \binom{[b]}{a}$ such that, for $i = 1, \dots, b$, we have $I_{i+1} \supset I_i \setminus \{i\}$. (Here the indices are taken modulo b , so that $I_1 \supset I_b \setminus \{b\}$.) Thus, if $i \notin I_i$, then $I_{i+1} = I_i$.

In other words, either $I_{i+1} = I_i$ or I_{i+1} is obtained from I_i by deleting i and adding another element. Note that if $I_{i+1} = I_i$, then either i belongs to all elements I_j of the necklace, or i belongs to none of them.

Example 7.13.7. The sequence $\mathcal{I} = (126, 236, 346, 456, 156, 126)$ is a Grassmann necklace of type $(3, 6)$.

Definition 7.13.8. For $\ell \in \{1, \dots, b\}$, we define the linear order $<_\ell$ on $\{1, \dots, b\}$ as follows:

$$\ell <_\ell \ell + 1 <_\ell \ell + 2 <_\ell \dots <_\ell b <_\ell 1 <_\ell \dots <_\ell \ell - 1.$$

For a decorated permutation $\tilde{\pi}$ on b letters, we say that $i \in \{1, \dots, b\}$ is an ℓ -anti-excedance of $\tilde{\pi}$ if either $\tilde{\pi}^{-1}(i) >_\ell i$ or if $\tilde{\pi}(i) = \bar{i}$. Thus, a 1-anti-excedance is the same as an (ordinary) anti-excedance, as in Definition 7.9.1.

It is not hard to see that the number of ℓ -anti-excedances does not depend on the choice of $\ell \in \{1, \dots, b\}$, so we simply refer to this quantity as the number of anti-excedances.

Lemma 7.13.9. *Decorated permutations on b letters with a anti-excedances are in bijection with Grassmann necklaces \mathcal{I} of type (a, b) .*

Proof. To go from \mathcal{I} to the corresponding decorated permutation $\tilde{\pi} = \tilde{\pi}(\mathcal{I})$, we set $\tilde{\pi}(i) = j$ whenever $I_{i+1} = (I_i \setminus \{i\}) \cup \{j\}$ for $i \neq j$. If $i \notin I_i = I_{i+1}$ then $\tilde{\pi}(i) = \bar{i}$, and if $i \in I_i = I_{i+1}$ then $\tilde{\pi}(i) = \bar{i}$.

Going in the other direction, let $\tilde{\pi}$ be a decorated permutation. For $\ell \in \{1, \dots, b\}$, we denote by I_ℓ the set of ℓ -anti-excedances of $\tilde{\pi}$. Then $\mathcal{I} = \mathcal{I}(\tilde{\pi}) = (I_1, \dots, I_b)$ is the corresponding Grassmann necklace. \square

Example 7.13.10. Let $\mathcal{I} = (126, 236, 346, 456, 156, 126)$, cf. Example 7.13.7. Then $\tilde{\pi}(\mathcal{I}) = (3, 4, 5, 1, 2, \bar{6})$.

Example 7.13.11. Let $\tilde{\pi}_G = \tilde{\pi}_{a,b}$, cf. (7.10.1). The corresponding Grassmann necklace (cf. Lemma 7.13.9) is given by

$$(7.13.1) \quad \mathcal{I}(\tilde{\pi}_{a,b}) = (\{1, 2, \dots, a\}, \{2, 3, \dots, a, a+1\}, \dots, \{b, 1, 2, \dots, a-1\}).$$

Definition 7.13.12. We extend the linear order $<_\ell$ on $\{1, \dots, b\}$ to a partial order on $\binom{[b]}{a}$, as follows. Let

$$\begin{aligned} I &= \{i_1, \dots, i_a\}, & i_1 <_\ell i_2 <_\ell \dots <_\ell i_a; \\ J &= \{j_1, \dots, j_a\}, & j_1 <_\ell j_2 <_\ell \dots <_\ell j_a. \end{aligned}$$

Then, by definition, $I \leq_\ell J$ if and only if $i_1 \leq_\ell j_1, \dots, i_a \leq_\ell j_a$.

Definition 7.13.13. For a Grassmann necklace $\mathcal{I} = (I_1, \dots, I_b)$ of type (a, b) , we define the associated *positroid* $\mathcal{M}_{\mathcal{I}}$ by

$$\mathcal{M}_{\mathcal{I}} = \{J \in \binom{[b]}{a} \mid I_\ell \leq_\ell J \text{ for all } \ell \in \{1, \dots, b\}\}.$$

As we will see in Chapter 8, positroids are the (realizable) *matroids* that arise from full rank $a \times b$ matrices with all Plücker coordinate nonnegative. Abstractly, one may also define a *positively oriented matroid* to be an oriented matroid on $\{1, 2, \dots, b\}$ whose chirotope takes nonnegative values on any ordered subset $\{i_1 < \dots < i_a\}$. By [1], these two notions are the same, in other words, every positively oriented matroid is realizable.

Example 7.13.14. Let $\mathcal{I} = \mathcal{I}(\tilde{\pi}_{a,b})$, see (7.13.1). Then $\mathcal{M}_{\mathcal{I}} = \binom{[b]}{a}$, i.e., the positroid associated with \mathcal{I} contains all a -element subsets of $\{1, \dots, b\}$.

Definition 7.13.15. Two reduced plabic graphs are called *strongly equivalent* if they have the same sets of face labels.

We note that two plabic graphs which are connected via moves (M2) and (M3) are strongly equivalent.

Recall that $\mathcal{F}_{\text{target}}(G)$ denotes the collection of target-labels of faces of a reduced plabic graph G .

Theorem 7.13.16 ([19, Theorem 1.5]). *Fix a decorated permutation $\tilde{\pi}$ on b letters with a anti-excedances. Let \mathcal{I} be the corresponding Grassmann necklace of type (a, b) , cf. Lemma 7.13.9. Let $\mathcal{M}_{\mathcal{I}}$ be the associated positroid, cf. Definition 7.13.13. Then the map $G \mapsto \mathcal{F}_{\text{target}}(G)$ gives a bijection between*

- the strong equivalence classes of reduced plabic graphs G with decorated trip permutation $\tilde{\pi}_G = \tilde{\pi}$ and
- the collections $\mathcal{C} \subset \binom{[b]}{a}$ that are maximal (with respect to inclusion) among the weakly separated collections satisfying $\mathcal{I} \subseteq \mathcal{C} \subseteq \mathcal{M}_{\mathcal{I}}$.

Remark 7.13.17. Let $\mathcal{I} = \mathcal{I}(\tilde{\pi}_{a,b})$. Then $\mathcal{I} = \mathcal{I}(\tilde{\pi}_{a,b})$ is given by (7.13.1). Each of the b cyclically consecutive subsets in (7.13.1) is weakly separated from every other a -element subset of $\{1, \dots, b\}$, so every maximal weakly separated collection $\mathcal{C} \subset \binom{[b]}{a}$ must contain \mathcal{I} . Furthermore, $\mathcal{M}_{\mathcal{I}} = \binom{[b]}{a}$ (see Example 7.13.14), so any such \mathcal{C} automatically satisfies the inclusions $\mathcal{I} \subseteq \mathcal{C} \subseteq \mathcal{M}_{\mathcal{I}}$. We thus recover Theorem 7.13.4 as a special case of Theorem 7.13.16.

Bibliography

- [1] ARDILA, F., RINCÓN, F., AND WILLIAMS, L. Positively oriented matroids are realizable. *J. Eur. Math. Soc. (JEMS)* 19, 3 (2017), 815–833.
- [2] ARKANI-HAMED, N., BOURJAILY, J., CACHAZO, F., GONCHAROV, A., POSTNIKOV, A., AND TRNKA, J. *Grassmannian geometry of scattering amplitudes*. Cambridge University Press, Cambridge, 2016.
- [3] BOCKLANDT, R. Calabi-Yau algebras and weighted quiver polyhedra. *Math. Z.* 273, 1-2 (2013), 311–329.
- [4] BROOMHEAD, N. Dimer models and Calabi-Yau algebras. *Mem. Amer. Math. Soc.* 215, 1011 (2012), viii+86.
- [5] DANILOV, V. I., KARZANOV, A. V., AND KOSHEVOY, G. A. On maximal weakly separated set-systems. *J. Algebraic Combin.* 32, 4 (2010), 497–531.
- [6] EARLY, N. From weakly separated collections to matroid subdivisions. arXiv:1910.11522.
- [7] FOCK, V., AND GONCHAROV, A. Moduli spaces of local systems and higher Teichmüller theory. *Publ. Math. Inst. Hautes Études Sci.*, 103 (2006), 1–211.
- [8] FOMIN, S., IGUSA, K., AND LEE, K. Universal quivers. arXiv:2003.01244.
- [9] FOMIN, S., PYLYAVSKYY, P., SHUSTIN, E., AND THURSTON, D. Morsifications and mutations. arXiv:1711.10598.
- [10] GALASHIN, P. Plabic graphs and zonotopal tilings. *Proc. Lond. Math. Soc. (3)* 117, 4 (2018), 661–681.
- [11] HARER, J. L. The virtual cohomological dimension of the mapping class group of an orientable surface. *Invent. Math.* 84, 1 (1986), 157–176.
- [12] HATCHER, A. On triangulations of surfaces. *Topology Appl.* 40, 2 (1991), 189–194.
- [13] KAWAMURA, T. Links associated with generic immersions of graphs. *Algebr. Geom. Topol.* 4 (2004), 571–594.
- [14] KENYON, R. An introduction to the dimer model. In *School and Conference on Probability Theory*, ICTP Lect. Notes, XVII. Abdus Salam Int. Cent. Theoret. Phys., Trieste, 2004, pp. 267–304.
- [15] KNUTSON, A., LAM, T., AND SPEYER, D. E. Positroid varieties: juggling and geometry. *Compos. Math.* 149, 10 (2013), 1710–1752.

- [16] KODAMA, Y., AND WILLIAMS, L. KP solitons and total positivity for the Grassmannian. *Invent. Math.* 198, 3 (2014), 637–699.
- [17] KODAMA, Y., AND WILLIAMS, L. K. KP solitons, total positivity, and cluster algebras. *Proc. Natl. Acad. Sci. USA* 108, 22 (2011), 8984–8989.
- [18] LECLERC, B., AND ZELEVINSKY, A. Quasicommuting families of quantum Plücker coordinates. In *Kirillov’s seminar on representation theory*, vol. 181 of *Amer. Math. Soc. Transl. Ser. 2*. Amer. Math. Soc., Providence, RI, 1998, pp. 85–108.
- [19] OH, S., POSTNIKOV, A., AND SPEYER, D. E. Weak separation and plabic graphs. *Proc. Lond. Math. Soc. (3)* 110, 3 (2015), 721–754.
- [20] OH, S. H., AND SPEYER, D. E. Links in the complex of weakly separated collections. *J. Comb.* 8, 4 (2017), 581–592.
- [21] POSTNIKOV, A. Total positivity, Grassmannians, and networks, [arXiv:math/0609764](https://arxiv.org/abs/math/0609764).
- [22] POSTNIKOV, A. Positive Grassmannian and polyhedral subdivisions. In *Proceedings of the International Congress of Mathematicians—Rio de Janeiro 2018. Vol. IV. Invited lectures* (2018), World Sci. Publ., Hackensack, NJ, pp. 3181–3211.
- [23] STANLEY, R. P. *Enumerative combinatorics. Vol. 1*, second ed., vol. 49 of *Cambridge Studies in Advanced Mathematics*. Cambridge University Press, Cambridge, 2012.
- [24] THURSTON, D. P. From dominoes to hexagons. In *Proceedings of the 2014 Maui and 2015 Qinhuangdao conferences in honour of Vaughan F. R. Jones’ 60th birthday* (2017), vol. 46 of *Proc. Centre Math. Appl. Austral. Nat. Univ.*, Austral. Nat. Univ., Canberra, pp. 399–414. Preprint versions: [arXiv:math/0405482](https://arxiv.org/abs/math/0405482) (2004 and 2016).
- [25] WILLIAMS, L. K. Enumeration of totally positive Grassmann cells. *Adv. Math.* 190, 2 (2005), 319–342.
- [26] WILLIAMS, L. K. A positive Grassmannian analogue of the permutohedron. *Proc. Amer. Math. Soc.* 144, 6 (2016), 2419–2436.